



Keywords:
Effective dose equivalent
Radiation exposure
Radiation protection
Photon radiation
Dosimetry
10 CFR 20

EPRI TR-101909
Volume 1
Project 3099-10
Final Report
February 1993

Assessment of the Effective Dose Equivalent for External Photon Radiation

Volume 1: Calculational Results for Beam and Point Source Geometries

Prepared by
Texas A&M University
College Station, Texas

Assessment of the Effective Dose Equivalent for External Photon Radiation

Volume 1: Calculational Results for Beam and Point Source Geometries

As of January 1994, U.S. nuclear plants must determine radiation exposure to their work force using a risk-based methodology termed "effective dose equivalent" (EDE). This report explains the EDE concept and describes the improved EPRI methodology for determining an EDE from conventional dosimetry measurements of radiation exposure.

INTEREST CATEGORIES

Nuclear plant operations and maintenance
Occupational radiation control
Radioactive waste management

KEYWORDS

Effective dose equivalent
Radiation exposure
Radiation protection
Photon radiation
Dosimetry
10 CFR 20

BACKGROUND In 1977, the International Commission on Radiological Protection (ICRP) introduced the concept of risk-based radiation dose limits. This concept was based on the fact that human organs and tissues differ in their susceptibility to the effects of radiation. To account for these organ differences, the ICRP proposed specific organ radiation exposure weighting factors. These and other aspects of the ICRP recommendations were adopted in revisions made in 1991 to 10 CFR 20. The regulations require licensees to evaluate radiation exposures in terms of the EDE using the conservative assumption that the weighting factor for external exposure is one. However, the regulations allow licensees to propose alternative methods for evaluating the external radiation component of an EDE. This report describes the enhanced approach EPRI is developing to evaluate EDEs.

OBJECTIVE To describe the EDE concept and explain the enhanced EPRI methodology for utility use in determining work force EDE.

APPROACH Researchers applied a validated and verified Monte Carlo computer code to calculate photon transport through the human body. They used mathematical models of the human adult male and female and—for a variety of external radiation sources—calculated energy deposition in a large number of human organs and tissues. Finally, given published organ weighting factors, they calculated EDEs for these irradiations.

RESULTS The mathematical models of the human body and the computer code used to calculate external photon interactions with the body functioned correctly. This allowed researchers to determine the dose equivalent to organs and tissues, and it facilitated correct weighting and summing of doses to ascertain the EDEs.

This report describes how the EDE varies with photon energy for various radiation beam source and point source geometries. Beam sources striking the front of the body normal to the body's major axis (straight on) produce the highest EDE. Beams striking the rear of the torso, again normal to the body's major axis, produce the next-highest EDE. For point sources in contact with the body, the EDE is highest for females when the source is on the front of the torso near the sternum. For males, the EDE is highest when the point source is on the front of the torso near the gonads. This report also discusses the relationship between an EDE and the location of dosimeters on the body and illustrates that dosimeter response to

off-normal radiation beams—those that do not strike the body straight on—will not underestimate the EDE. Volume 1 of this report describes the EDE concept, evolution, incorporation into regulations, and calculations for a broad range of photon energies and radiation source geometries. Volume 2, due in late 1993, will describe ongoing work to develop algorithms that will improve the methods for determining an EDE using conventional dosimeters.

EPRI PERSPECTIVE U.S. nuclear utilities should develop a technically rigorous approach for determining EDEs for their work forces. Such an approach should be generally conservative, acceptable to regulatory agencies, and consistent with existing dosimetry practices. This report presents a methodology for meeting those objectives. EPRI will continue to work closely with member utilities, industry groups, and regulators to review, verify, and validate this methodology. Overall, EPRI's goal is a more accurate EDE methodology that uses conventional dosimetry measurements of radiation exposure.

PROJECT

RP3099-10

Project Manager: Carol Hornibrook

Nuclear Power Division

Contractor: Texas A&M University

For further information on EPRI research programs, call
EPRI Technical Information Specialists (415) 855-2411.

Assessment of the Effective Dose Equivalent for External Photon Radiation

Volume 1: Calculational Results for Beam and Point Source Geometries

**TR-101909, Volume 1
Research Project 3099-10**

Final Report, February 1993

Prepared by
TEXAS A&M UNIVERSITY
College Station, Texas 77843-3133

Principal Investigators
W. D. Reece
J. W. Poston
X. G. Xu

Prepared for
Electric Power Research Institute
3412 Hillview Avenue
Palo Alto, California 94304

EPRI Project Manager
C. Hornibrook

Low Level Waste and Coolant Technology Program
Nuclear Power Division

DISCLAIMER OF WARRANTIES AND LIMITATION OF LIABILITIES

THIS REPORT WAS PREPARED BY THE ORGANIZATION(S) NAMED BELOW AS AN ACCOUNT OF WORK SPONSORED OR COSPONSORED BY THE ELECTRIC POWER RESEARCH INSTITUTE, INC. (EPRI). NEITHER EPRI, ANY MEMBER OF EPRI, ANY COSPONSOR, THE ORGANIZATION(S) NAMED BELOW, NOR ANY PERSON ACTING ON BEHALF OF ANY OF THEM:

(A) MAKES ANY WARRANTY OR REPRESENTATION WHATSOEVER, EXPRESS OR IMPLIED, (I) WITH RESPECT TO THE USE OF ANY INFORMATION, APPARATUS, METHOD, PROCESS, OR SIMILAR ITEM DISCLOSED IN THIS REPORT, INCLUDING MERCHANTABILITY AND FITNESS FOR A PARTICULAR PURPOSE, OR (II) THAT SUCH USE DOES NOT INFRINGE ON OR INTERFERE WITH PRIVATELY OWNED RIGHTS, INCLUDING ANY PARTY'S INTELLECTUAL PROPERTY, OR (III) THAT THIS REPORT IS SUITABLE TO ANY PARTICULAR USER'S CIRCUMSTANCE; OR

(B) ASSUMES RESPONSIBILITY FOR ANY DAMAGES OR OTHER LIABILITY WHATSOEVER (INCLUDING ANY CONSEQUENTIAL DAMAGES, EVEN IF EPRI OR ANY EPRI REPRESENTATIVE HAS BEEN ADVISED OF THE POSSIBILITY OF SUCH DAMAGES) RESULTING FROM YOUR SELECTION OR USE OF THIS REPORT OR ANY INFORMATION, APPARATUS, METHOD, PROCESS, OR SIMILAR ITEM DISCLOSED IN THIS REPORT.

ORGANIZATION(S) THAT PREPARED THIS REPORT:

TEXAS A&M UNIVERSITY

ORDERING INFORMATION

Requests for copies of this report should be directed to the EPRI Distribution Center, 207 Coggins Drive, P.O. Box 23205, Pleasant Hill, CA 94523, (510) 934-4212. There is no charge for reports requested by EPRI member utilities and affiliates.

Electric Power Research Institute and EPRI are registered service marks of Electric Power Research Institute, Inc.

Copyright © 1993 Electric Power Research Institute, Inc. All rights reserved.

ABSTRACT

Beginning in January 1994, U.S. nuclear power plants must change the way that they determine the radiation exposure to their workforce. At that time, revisions to Title 10 Part 20 of the Code of Federal Regulations will be in force requiring licensees to evaluate worker radiation exposure using a risk-based methodology termed the "effective dose equivalent." Effective dose equivalent is intended to be a measure of radiation exposure that represents an individual's risk of stochastic injury from that exposure, in particular the risk of fatal cancer or genetic defects in his or her progeny. Effective dose equivalent is based on the known variations in sensitivity to radiation of the various organs of the body. By accounting for these variations, effective dose equivalent will yield a measure of radiation exposure that is proportional to risk.

A research project was undertaken to improve upon the conservative method presently used for assessing effective dose equivalent. In this project effective dose equivalent was calculated using a mathematical model of the human body, and tracking photon interactions for a wide variety of radiation source geometries using Monte Carlo computer code simulations. Algorithms were then developed to relate measurements of the photon flux on the surface of the body (as measured by dosimeters) to effective dose equivalent. This report (Volume I of a two-part study) describes:

- the concept of effective dose equivalent
- the evolution of the concept and its incorporation into regulations
- the variations in human organ susceptibility to radiation
- the mathematical modeling and calculational techniques used
- the results of effective dose equivalent calculations for a broad range of photon energies and radiation source geometries.

The study determined that for beam radiation sources the highest effective dose equivalent occurs for beams striking the front of the torso. Beams striking the rear of the torso produce the next highest effective dose equivalent, with effective dose equivalent falling significantly as one departs from these two orientations. For point sources, the highest effective dose equivalent occurs when the sources are in contact with the body on the front of the torso. For females the highest effective dose equivalent occurs when the source is on the sternum, for males when it is on the gonads.

This body of work, when combined with the next phase of the project (which will include photon surface flux calculations, results of experimental measurements made on physical models of the human torso, and conventional dosimeter measurements of radiation exposure), provides the data needed to better assess effective dose equivalent for nuclear power plant workers.

ACKNOWLEDGMENTS

Thank you to Kevin Braby and Brenda Mooney of Texas A&M University for software development and manuscript preparation, respectively.

The following individuals served as technical advisors to EPRI for this project, and as such reviewed the manuscript and made many helpful recommendations:

- Robert E. Alexander (The Alexander Corporation)
- Ralph Andersen (NUMARC)
- John J. Kelly (New York Power Authority)
- Michael D. Naughton (TARAwest)
- Dennis E. Owen (ENCORE Technical Resources, Inc.)
- John Schmitt (NUMARC)
- John Trejo (Public Service Electric & Gas)
- Michael Williams (Union Electric Company)

CONTENTS

Section	Page
1 Introduction	1-1
1.1 The Purpose of This Study	1-1
1.2 Background	1-1
1.3 Definition of Terms	1-3
1.4 Approaches of External Dosimetry	1-3
1.5 Report Organization	1-4
2 Estimating the Effective Dose Equivalent	2-1
2.1 The Theoretical Basis for Assessing External Dose	2-1
2.2 Modeling the Human Body	2-3
2.2.1 The Mathematical Models	2-3
2.2.2 Organ Weighting Factors	2-3
2.3 The Photon Transport Computer Code	2-6
3 The Results of the Effective Dose Equivalent Calculations	3-1
3.1 Overview of the EDE Calculations	3-1
3.2 Beam Source Results	3-1
3.3 Point Source Results	3-5
3.3.1 Results With Point Sources in Contact With the Torso	3-13
3.3.2 Results With Point Sources Away From the Torso	3-15
4 Conclusions and Future Work	4-1
4.1 Conclusions of Phase I	4-1
4.2 Future Work	4-22
5 References	5-1
Attachment 1: Supporting Graphics and Tables	A1-1

Appendix A: Computer Input Deck Describing the Male and Female Phantoms

Appendix B: One-Page Summary Sheets for the MCNP Calculations for Beam Geometries

Appendix C: One-Page Summary Sheets for the MCNP Calculations for Point Source Geometries

Appendices are on IBM compatible disks available from the EPRI Distribution Center.

LIST OF FIGURES

Figure	Page
1 Energy flux balance over a differential volume	2-2
2 Exterior of the adult male phantom	2-4
3 Typical model of a portion of the human body	2-5
4 Nomenclature used to describe the beam angle of incidence	3-2
5 Phantom irradiation geometries	3-3
6 Effective dose equivalent vs. photon energy for beam geometries	3-4
7 Effective dose equivalent vs. azimuthal angle	3-6
8 Effective dose equivalent vs. polar angle	3-7
9 Surface and contour plots of effective dose equivalent for a male for 1.0 MeV photon beams	3-11
10 Surface and contour plots of effective dose equivalent for a female for 1.0 MeV photon beams	3-12
11 Flux-to-dose conversion factors	3-13
12 Schematic of the phantom coordinate system	3-14
13 Contour plots of H_E for 1.0 MeV point sources in contact with the body (units = 10^{-15} rem/photon emitted)	3-19
14 Surface plots of H_E for a female vs. source location for a 1.0 MeV point source	3-20
15 Surface plots of H_E for a male vs. source location for a 1.0 MeV point source	3-21
16 Contour plots of H_E for a female vs. source location for a 1.0 MeV point source	3-22
17 Contour plots of H_E for a male vs. source location for a 1.0 MeV point source	3-22

LIST OF TABLES

Table		Page
1	Organ Dose Weighting Factors	1-3
2	Gender-Specific Organ Weighting Factors (w_T)	2-6
3	Remainder Organs	2-6
4	Effective Dose Equivalent Comparison of This Study With ICRP-51	3-4
5	Effective Dose Equivalent for 0.08 MeV Photon Beams as a Function of Polar and Azimuthal Angle (units = E-10 rem-sq cm)	3-8
6	Effective Dose Equivalent for 0.3 MeV Photon Beams as a Functions of Polar and Azimuthal Angle (units = E-10 rem-sq cm)	3-9
7	Effective Dose Equivalent for 1.00 MeV Photon Beams as a Function of Polar and Azimuthal Angle (units = E-10 rem-sq cm)	3-10
8	Effective Dose Equivalent as a Function of Point Source Location on the Torso (0.08 MeV Photons, units = rem per photon x E-15)	3-16
9	Effective Dose Equivalent as a Function of Point Source Location on the Torso (0.03 MeV Photons, units = rem per photon x E-15)	3-17
10	Effective Dose Equivalent as a Function of Point Source Location on the Torso (1.0 MeV Photons, units = rem per photon x E-15)	3-18

1

INTRODUCTION

1.1 The Purpose of This Study

The work reported herein is the culmination of several years of research sponsored by the Electric Power Research Institute (EPRI). EPRI undertook this research on behalf of its member utilities to help them prepare for some fundamental changes being made in federal radiation protection regulations. Title 10 Part 20 of the Code of Federal Regulations ("Standards for Protection Against Radiation") was revised in 1991.¹ The revised regulations codify the long-standing practice of requiring licensees to ensure that radiation exposure is maintained as low as is reasonably achievable. The regulations add, however, the concept of "effective dose equivalent," and require that certain effective dose equivalent limits not be exceeded. This last requirement is the subject of this report.

The precise definition of effective dose equivalent is discussed in Section 1.3. For the moment, consider effective dose equivalent to be a radiation protection philosophy based on:

- the observation that radiation can cause stochastic (random) effects in the human body (such as cancer in the recipient of the radiation or genetic defects in his or her progeny or in subsequent generations)
- the observation that human organs and tissues differ in their susceptibility to stochastic effects.

Thus, when effective dose equivalent is determined the variations in organ susceptibility should be considered. If one correctly considers these radiation susceptibility variations, then the dose is not just an average exposure to the body as measured by one or more dosimeters. Instead the resultant value—the effective dose

equivalent—is truly proportional to the risk of stochastic injury by that particular radiation exposure event.

Practically, one cannot place dosimeters over the body's entire surface or inside individual organs in order to measure ionizing radiation. Rather, one must use calculational methods—algorithms—to evaluate effective dose equivalent from the combined effects of external and internal radiation sources. To assess the risk of radiation to organs and tissues one must know where the radiation is emanating from, the properties of that radiation (type, energy, etc.), the organs' differing sensitivities to radiation, and the shielding effects of the body itself. This knowledge—coupled with a small number of actual measurements at discrete locations on the body (for external exposures) or airborne concentrations or bioassay measurements (for internal exposures)—makes it possible to estimate total effective dose equivalent. The purpose of this study was to develop a technique to estimate effective dose equivalent for external radiation that could be adopted by utilities and be acceptable to the Nuclear Regulatory Commission (NRC).

1.2 Background

This research had its origins in a 1977 publication by the International Commission on Radiological Protection (ICRP).² That publication—ICRP-26—introduced a variety of new radiation protection concepts, including the concept of risk-based dose limits for stochastic effects. It also proffered the idea that workers exposed to radiation should have approximately the same risk of injury as workers in other "safe" industries who were not exposed to radiation. For stochastic effects (such as cancer) the ICRP recommended that exposure limits should apply to the sum of the doses to the individual organs

(or tissues) of the body. They also specified the weighting factors to be applied to the individual organ doses to account for differences in cellular radio-sensitivity, variations in susceptibility to stochastic effects, and variations in the treatability and lethality of different cancers. (The technique used to calculate the weighting factors is described in Reference 3.) This new approach also supports the principle that risk should be equal, whether the body is irradiated uniformly or receives localized irradiation. In addition, this approach has the advantage that as radiation effects knowledge improves, weighting factors can be periodically updated.

To understand the weighting factor effect, consider the following example. Imagine a situation (say a medical treatment) where all of the radiation was received by a single organ or tissue. In the case of one individual it was the bone, in the case of another it was the lungs. Now the weighting factor assigned by the ICRP to these organs is 0.03 for the bone surfaces and 0.12 for the lungs. This means that the bone patient can receive four times the radiation dose of the lung patient, and both will have the same risk of death from cancer from their treatments.

The ICRP recommendations for organ and tissue weighting factors were adopted when the radiation protection standards of 10 CFR 20 were revised in 1991. These revised regulations, scheduled to become effective no later than January 1, 1994, specify that a worker's annual total effective dose equivalent must not exceed 5 rem. (Other limits—including doses to an individual organ, to the lens of the eye, and to the skin—are also specified, but they are not applicable to this discussion.) The regulations require that total effective dose equivalent be calculated by summing the external component (inconsistently called by various terms, including deep-dose equivalent* and dose equivalent) and the internal component (called the committed** effective dose equivalent). As explained in the revised regulations, the published weighting factors are intended to be used for weighting the *internal* dose to organs and tissues. In the weighting factor table the regulations specify that a single weighting factor equal to unity be used for the "whole body" (a tissue not specified in ICRP-26) when calculating the *external* component of the total effective dose equivalent.

* The dose equivalent at a tissue depth of 1 cm (1,000 mg/cm²).

** The term "committed" is used because internal radiation "commits" the body to receiving future exposure, and this future exposure must be accounted for.

When the NRC proposed a whole body weighting factor equal to unity, they perhaps recognized that this calculation method was simplistic, and would not yield an accurate (true risk-based) effective dose equivalent. Nonetheless, they apparently were not prepared to recommend a more accurate calculational approach. They did recognize, however, that licensees would want to develop more accurate techniques for measuring external exposure. Accordingly, they added the following sentence⁴ to a footnote prescribing that an external weighting factor of one be used:

The use of other weighting factors for external exposure will be approved on a case-by-case basis until such time as specific guidance is issued.

An NRC Regulatory Guide⁵ was subsequently issued, but it primarily addresses internal dose calculations and does not suggest alternative approaches to external dose.

This then is the purpose of the research reported here: to develop a calculation technique for accurately assessing the external component to total effective dose equivalent from ionizing photon radiation (x- and gamma rays, not charged particles or neutrons). Since the vast majority of exposures at nuclear power plants involve external exposures only, accurate (and not excessively conservative) estimates of these exposures are particularly important to workers and utilities. Accurate effective dose equivalent exposure records will:

- provide a basis for optimizing worker protection practices
- provide meaningful data for ongoing evaluations of radiation exposure risks.

An effective dose equivalent estimation technique must be able to be readily used by utilities and must be acceptable to the NRC. Utility acceptance will require that the technique be accurate, consistent with existing dosimetry practices, and straightforward to implement. The technique must meet a variety of criteria for NRC acceptance, but above all it must be technically rigorous. EPRI believes that the effective dose equivalent methodology described herein meets the utility and NRC criteria.

1.3 Definition of Terms

The organ dose weighting factors (assigned the symbol w_T) specified in ICRP-26 and adopted in the revisions to 10 CFR 20 are listed in Table 1.

Table 1
Organ Dose Weighting Factors

Organ or Tissue	Weighting Factor (w_T)
Gonads	0.25
Breast	0.15
Lung	0.12
Red Bone Marrow	0.12
Thyroid	0.03
Bone Surfaces	0.03
Remainder	0.30

The "Remainder" category groups the other organs of the body, excluding the skin and the lens of the eye. The five organs in this category that receive the highest radiation exposure are each assigned a weighting factor of 0.06. By convention, the radiation exposure to the other remainder organs and tissues are neglected when determining the effective dose equivalent. In the actual weighting factor table published in 10 CFR 20, the "whole body" is also listed as an "organ" with $w_T = 1.0$. As explained above, this is the way the drafters of the regulations dealt with the fact that the listed weighting factors generally were applied only to radiation exposures from internal emitters, yet the regulations must also be applicable to external exposures (so that the internal and external doses can be summed to yield the estimated effective dose equivalent).

At this point it is appropriate to comment briefly on the magnitude of the errors in external radiation dose that are introduced with the assumption that $w_T = 1.0$, and why it is so important that a more technically rigorous approach be adopted. For irradiation by ^{60}Co , the absorbed dose to an organ 10 cm deep into the body is lower than the absorbed dose 1 cm deep. For ^{137}Cs the absorbed dose is substantially lower yet. Clearly, assigning the dose at the highest dose point on the torso to all the organs

significantly overestimates the external component of effective dose equivalent under many circumstances. Thus, for those (very common) instances when internal exposures are absent, this assumption means that the radiation worker's risk of stochastic injury is also dramatically overestimated. One of the functions of this report is provide an alternative to this overestimation, and to provide a mechanism to equate risk assessment from internal and external exposures.

Before describing that mechanism in more detail in the next section, it is important to define the principal radiation exposure terms used in this report.

- Mean dose equivalent: The average absorbed dose to an organ or tissue multiplied by the quality factor (Q) for the type of radiation. For gamma radiation (the penetrating type routinely encountered in the nuclear power industry), $Q = 1.0$. The mean dose equivalent to an organ or tissue is assigned the symbol H_T .
- Effective dose equivalent: The effective dose equivalent is the sum of the products of the mean dose equivalents to organs and tissues and the weighting factors. The effective dose equivalent is an indicator of the risk of death or serious genetic defects (in the first two generations) from ionizing radiation exposure. The effective dose equivalent is assigned the symbol H_E .

The total effective dose equivalent is the sum of the effective dose equivalents for the individual organs and tissues (designated by the subscript i) multiplied by their respective weighting factors. That is:

$$H_E = \sum H_{Ei} = \sum w_{Ti} \times H_{Ti} \quad (\text{Eq. 1})$$

1.4 Approaches to External Dosimetry

The current nuclear industry external dosimetry practice is to assign a "whole body dose" to individual workers based on measurements obtained from personal dosimeters. Often only one dosimeter is worn, generally on the chest. If multiple dosimeters are worn it is common practice to assign the highest measured radiation reading to be the "whole body dose." This assures that the worker's radiation exposure is never underestimated, though it has the obvious disadvantage of often overestimating the actual exposure.

One approach to determining a worker's effective dose equivalent from external radiation sources would be to have complete knowledge of the radiation fields producing the exposure and detailed knowledge of dose distributions within the body, particularly to those organs and tissues known to be at risk. Current dosimeters have several detection elements that allow the radiation field to be separated into penetrating and non-penetrating components, and allow a dose to be assigned to both components. However, they provide no information on the geometry of the source or of doses to key organs. The challenge is to take one (or at most a few) dosimeter measurements and from them estimate the worker's effective dose equivalent.

One can use either an experimental or calculational approach to solving this problem. Realistic physical models representing the human body (termed "phantoms") have been used for years for radiation exposure experiments. (They are discussed in more detail in Section 2.2.) In principle, it is possible to imagine conducting an extremely large number of phantom irradiation experiments to determine effective dose equivalent. The critical organs and tissues within the phantoms would be monitored with dosimeters, and one (or a few) dosimeters would be placed on the surface of the phantom. These latter dosimeters would be placed at those locations where radiation workers commonly wear their dosimeters (chest, waist, head, etc.). Hundreds or perhaps thousands of irradiation experiments would have to be performed on both male and female phantoms to study variables such as the type of radiation, the energy spectrum, the angular and spatial distribution of the incident radiation, the orientation of the body in the radiation field, etc. Only then would one have an adequate database, such that a worker's actual dosimeter measurement(s) could be converted to his or her external effective dose equivalent value. The number of sophisticated phantoms needed, the complexity of the measurements, and the experiment time required makes such an approach impractical and too expensive.

With the development of high-speed computers, most dosimetrists have taken a calculational approach to solving these problems. Mathematical modeling has been

shown to be a powerful yet flexible approach to solving both external and internal dosimetry problems. Indeed, many of the physical parameters used for the calculations are known to far better precision than the accuracy of the field instruments that would be used to make experimental measurements. In this approach, the human body is mathematically modeled and the behavior of a very large number of incident photons striking the body are calculated. Most often so-called Monte Carlo* methods are used to track and sum the photon behavior. This approach requires both a detailed knowledge of the photon interaction processes within tissues and an accurate organ model. Even though photon interaction processes are well understood and accurate mathematical descriptions of the body have been developed, it is common practice to confirm the calculations with a limited series of experiments.

This then is the approach taken in this study. First, model the human body. Second, use a Monte Carlo computer code to calculate effective dose equivalent to individual organs and tissues from a variety of radiation sources and source geometries. Third, for these same radiation sources and geometries, calculate the photon surface flux for those locations on the body at which dosimeters are usually placed. Fourth, mathematically relate the effective dose equivalents to the surface flux values, and then generalize the process so that it can be done in reverse. That is, derive algorithms that will allow personal dosimeter measurements (in essence, surface flux values) to be converted to effective dose equivalents. And finally, perform a series of irradiation experiments on physical phantoms and evaluate how accurately the algorithms predict the experimental measurements.

1.5 Report Organization

This Introduction is followed by Section 2.0 describing the calculational approach in greater detail. It reviews the theory of external dose assessment, describes in detail the human body models used in the study, and presents the computer code used in the calculations. Section 3.0 presents the results of the effective dose equivalent calculations—in tabular and graphical form—for both beam sources and point sources of radiation. Conclusions and recommendations from the beam and point

* In this case the Monte Carlo code would calculate the transport of photons within the body. By calculating the statistical behavior of a very large number of photons, the dose at discrete locations can be evaluated. The name "Monte Carlo" stems from the use of a random number generator in the code.

source calculations are presented in Section 4.0. This report is the first in a series of two EPRI reports on effective dose equivalent. The subsequent report (Volume II, to be published in 1993) will address:

- photon surface flux calculations
- recommended algorithms to convert dosimeter values to H_E
- the results of irradiation experiments on phantoms performed in actual power plant radiation fields.

Section 4.0 also briefly describes this future work (most of which is presently completed and is being analyzed) and discusses how the two reports may be used by the nuclear industry to determine effective dose equivalents that are both technically meaningful and accurate.

2

ESTIMATING THE EFFECTIVE DOSE EQUIVALENT

2.1 The Theoretical Basis for Assessing External Dose

In this section we present a brief mathematical derivation of one of the critical principles underlying this study: knowing certain properties of the radiation flux at the surface of the body allows doses within the body to be estimated. Those readers not interested in the mathematics of the derivation should nonetheless realize that several important concepts are imbedded in the derivation:

- Radiation fields can be described in units of energy current, that is the directional photon intensity times the energy of the photon. The units of energy current are $\text{MeV}/\text{cm}^2\text{-s}$.
- The change in energy current per unit time in all directions—what is mathematically termed the divergence in energy current—is the dose rate, and the divergence in energy current at a point is the dose.
- The average dose at a point within a volume can be expressed as a function of the energy current passing through a unit surface of that volume, and of the incident angle of that current. That is, knowing the photon flux at the surface allows the dose at a point in the underlying volume to be calculated.

Consider an object exposed to an electromagnetic field which penetrates the object and interacts with the material comprising the object. If the field is described in units of energy current, i.e., the directional photon intensity times the energy of the photon, having the units of $\text{MeV}/\text{cm}^2\text{-s}$, then a balance can be made along the x-direction

visualizing a small volume within the object as shown in Figure 1. The change per unit time in the energy density between the two faces of the cube at $x+\Delta x$ and x is energy current per unit time multiplied by the cross sectional area:

$$\Psi\Delta y\Delta z|_{x+\Delta x} - \Psi\Delta y\Delta z|_x =$$

$$\Delta E_x \text{ per unit volume per unit time across the } x \text{ faces} \quad (\text{Eq. 2})$$

where $|_x$ means evaluated at position x , Ψ is the energy current with units of $\text{MeV}/\text{cm}^2\text{-sec}$; and Δx , Δy , and Δz have units of cm ; and ΔE_x is the time change in energy density within the small volume. Similar balances made in the y - and z -directions, summed with the x -direction balance, give:

$$\begin{aligned} -\frac{dE}{dt}\Delta x\Delta y\Delta z = & (\Psi\Delta y\Delta z|_{x+\Delta x} - \Psi\Delta y\Delta z|_x) \\ & + (\Psi\Delta x\Delta z|_{y+\Delta y} - \Psi\Delta x\Delta z|_y) \\ & + (\Psi\Delta x\Delta y|_{z+\Delta z} - \Psi\Delta x\Delta y|_z) \end{aligned}$$

(Eq. 3)

where dE/dt is the time rate of change of energy in the differential volume.

Now divide Equation 3 by Δx , Δy , and Δz , and let Δx , Δy , and Δz approach zero. The right hand side of Equation 3 becomes, by definition, the partial derivative of Ψ in the x -, y -, and z -direction:

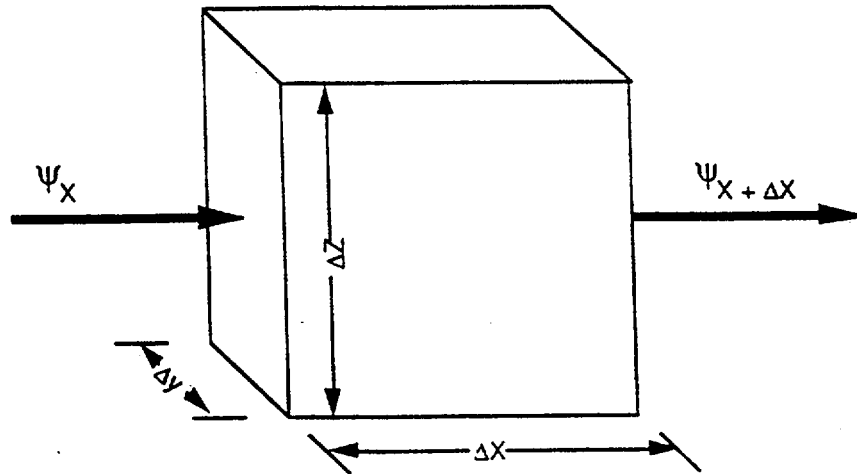


Figure 1. Energy flux balance over a differential volume

$$-\frac{dE}{dt} = \frac{\Psi_{x+\Delta x} - \Psi_x}{\Delta x} + \frac{\Psi_{y+\Delta y} - \Psi_y}{\Delta y} + \frac{\Psi_{z+\Delta z} - \Psi_z}{\Delta z} \quad (\text{Eq. 4})$$

or,

$$-\frac{dE}{dt} = \frac{\partial \Psi_x}{\partial x} + \frac{\partial \Psi_y}{\partial y} + \frac{\partial \Psi_z}{\partial z} \quad (\text{Eq. 5})$$

as Δx , Δy , and Δz approach zero.

The collection of the derivatives in all directions shown on the right hand side of Equation 5 is formally named the divergence. Using the standard vector calculus symbol for the divergence, ∇ , the equation reduces to a simple form:

$$-\frac{dE}{dt} = \nabla \cdot \Psi \quad (\text{Eq. 6})$$

In words, this equation states that the divergence of the energy current is equal to the change in energy density per unit time at a particular point. If there is no source in the object (i.e., all radiation originates outside the volume), all changes in the energy are losses within the volume. The energy lost from the field and deposited at a point is dose, by definition, and energy deposited at a point per unit time is dose rate. So, finally we see that Equation 6 states that divergence of the energy current at a point is equal to dose at that point per unit time.

If, as in the past, we were interested only in average dose, we could calculate the average dose rate over the object by:

$$\overline{\text{dose rate}} = \iiint \nabla \cdot \Psi dV \quad (\text{Eq. 7})$$

where $\overline{\text{dose rate}}$ is the average dose rate. But this expression can be reduced from a third order (or volume) integral to a second order (or surface) integral by using the "divergence theorem." The divergence theorem states that:

$$\iiint \nabla \cdot \Psi dV = \iint \mathbf{n} \cdot \Psi dS \quad (\text{Eq. 8})$$

where \mathbf{n} is the outwardly directed surface normal vector. From the divergence theorem, we see that the average dose is equal to the surface integral of the energy current multiplied by the cosine of the angle between the current and the surface normal (the vector dot product). Equation 8 can be solved directly using advanced numerical methods. These solutions—coupled with some specialized dosimetry—could be used to evaluate effective dose equivalent. It must be acknowledged, however, that the abstract mathematical nature and the need for specialized dosimetry would preclude wide industry acceptance. We have developed this result to show that the dose assessment approach described in this report

works not by accident, but as a natural consequence of the underlying radiation field theory. Realizing that the divergence of the energy current is dose leads, via the divergence theorem, directly to the concept that understanding fluxes at the surface of the body allows dose within the body to be estimated. This flux divergence approach also allows us to assess how accurate and reliable our procedures are for assessing effective dose equivalent based on surface flux measurements.

2.2 Modeling the Human Body

2.2.1 The Mathematical Models

A variety of mathematical models (or phantoms) of the human body have been developed, published, and are being used by the radiation protection community. The original models—published in the mid-1960s—were quite simple, and usually contained no internal organs or a limited set of crudely described key organs. The models have evolved over time and now are quite sophisticated. Phantoms of newborns through adults are available, and they model all of the major internal organs, and many other anatomical features. Both male and female phantoms are available, so that the genitals, breasts, and internal organ size and location differences can be accurately evaluated.

This study used the mathematical models developed by Cristy and Eckerman⁶, representing a standard adult male and female. Each phantom consists of three major sections (Figure 2):

- the trunk and arms (represented by an elliptical cylinder)
- the legs and feet (represented by two truncated circular cones)
- the head and neck (represented by an elliptical cylinder capped by half an ellipsoid).

The various structures within these sections are modeled geometrically and assigned one of three tissues: skeletal, lung, or soft tissue.

In the Cristy-Eckerman phantoms well over 150 organs and structures are modeled as a series of solid volumes that interconnect in various ways to approximate size, shape, and position of the organ. The published model consists of a large number of equations, each describing a particular anatomical feature of the phantom. These

equations are accompanied by tables that list the numerical factors and coefficients that are used in the equation to construct that particular feature. The tables present a range of coefficients so that male and female models spanning a variety of ages from newborn to adult can be created. Figure 3 gives the unfamiliar reader a good sense of how the mathematical phantoms are constructed.

The adult male and adult female modeled for this study weigh 71 and 56 kg respectively. The female model is based upon the model of a fifteen year old male, modified to include breasts, ovaries, and uterus representative of an adult female, and with slight adjustments to the placement of several internal organs. Minor changes in the published Cristy-Eckerman phantoms were made to account for small errors and discrepancies discussed in the literature since their original publication. The input deck describing the specific male and female mathematical models used in this study is presented in Appendix A. (Because of their length, the appendices for this report are contained on a computer disk supplied with the document.)

2.2.2 Organ Weighting Factors

Publication ICRP-26, which serves as the basis for 10 CFR 20, uses age- and gender-averaged weighting factors. The weighting factors used in these publications (repeated in Table 1 above) assume a population of 50% male and 50% female. While these assumptions simplify the process of evaluating exposure, they do not reflect reality. The nuclear power industry workforce is about 90% male and 10% female.⁷ Furthermore, it is known that the thyroids and breasts of women are more susceptible to the stochastic effects of ionizing radiation than those of men. In this study we made a deliberate decision to consider gender differences for several reasons. First, ICRP-51⁸ (a 1987 publication addressing protection against external radiation) acknowledges the importance of the issue. That study used gender-specific phantoms and calculated organ dose equivalents for both males and females. The publication states:

... the high risk coefficient for the female breast may be particularly important with external radiation and greatly influence the magnitude of the effective dose equivalent.

Second, by allowing for gender-specific calculations early, the labor involved was far less than if the entire

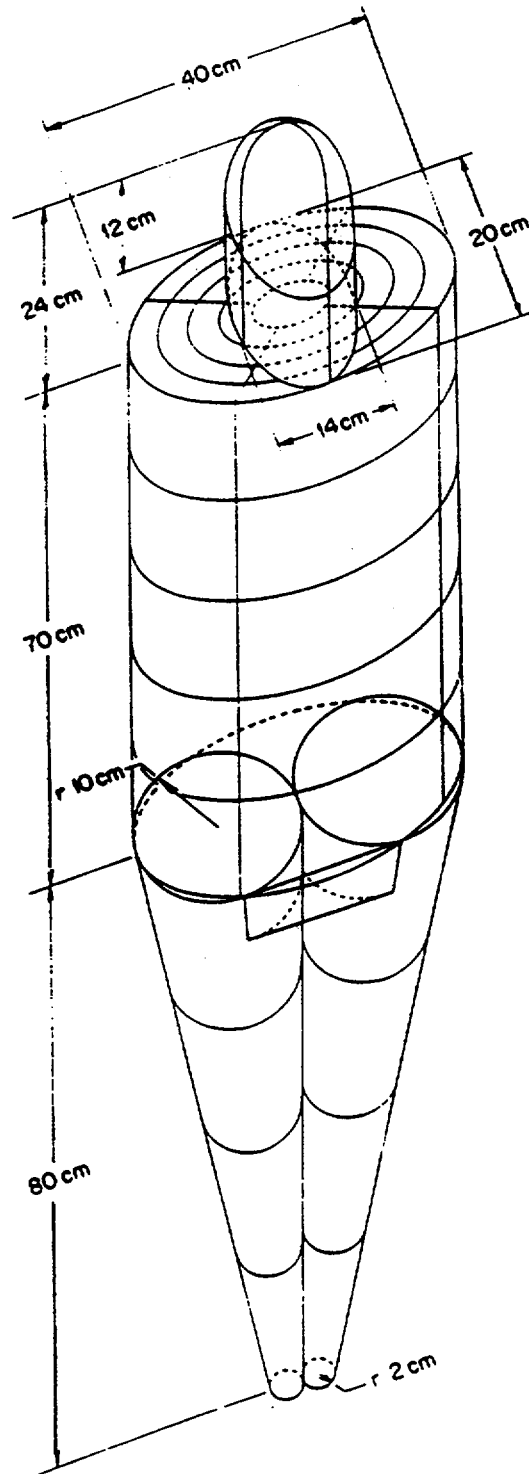


Figure 2. Exterior of the adult male phantom

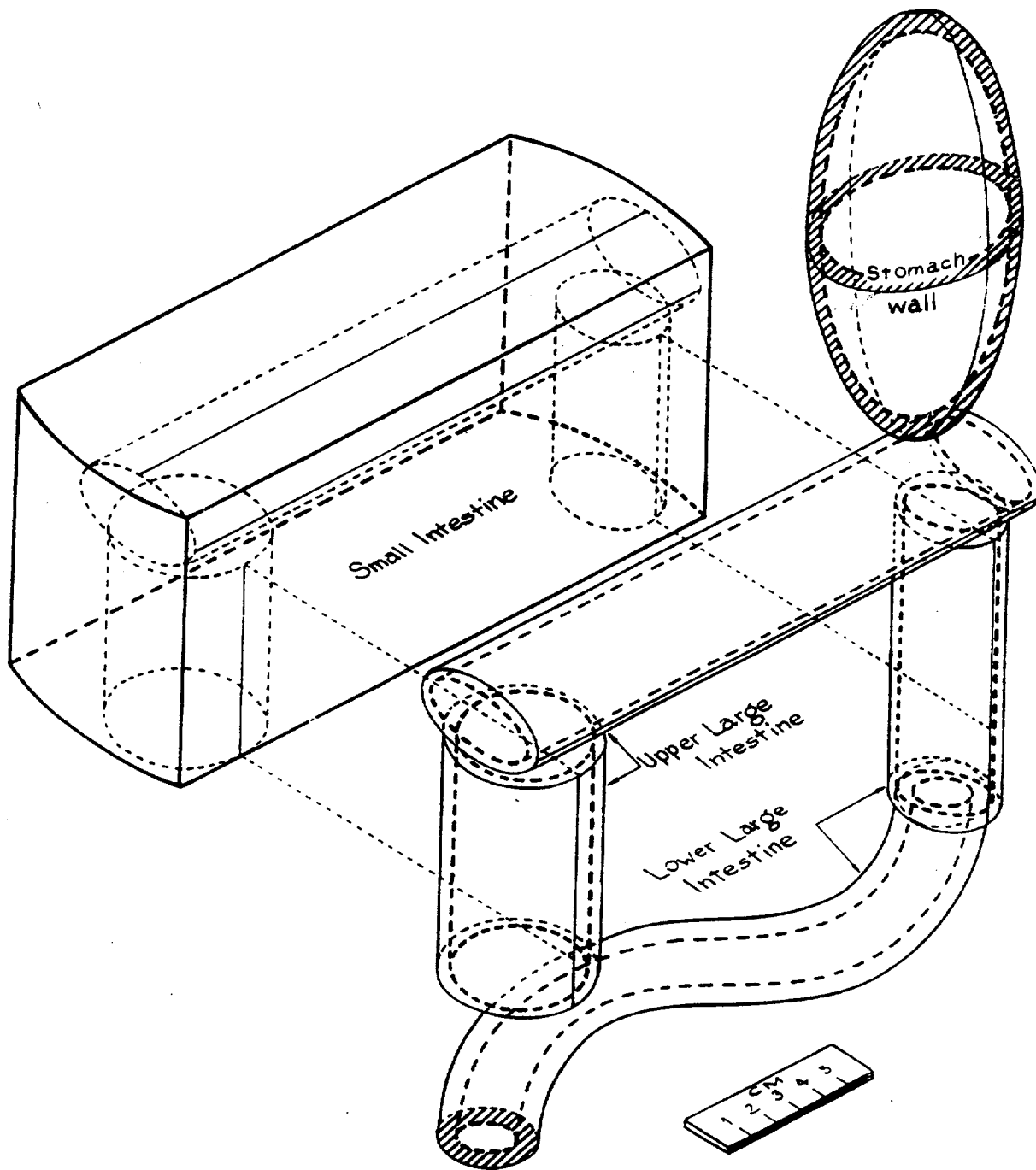


Figure 3. Typical model of a portion of the human body (Snyder, et. al., NUREG/CR-1159)

calculational process had to be set up and repeated sometime in the future.

Therefore, we chose to use gender-specific weighting factors even though such factors are not addressed in 10 CFR 20. The weighting factors we chose reduce to the values in 10 CFR 20 (and ICRP-26) when averaged over a standard 50% male-50% female population. The weighting factors we used are based on risk factors published by Kramer and Drexler⁹; they are shown in Table 2.

Table 2
Gender-Specific Organ Weighting Factors (w_T)

Organ	Male	Female	10 CFR 20
Gonads	0.25	0.25	0.25
Breast	0.00	0.30	0.15
Lung	0.12	0.10	0.12*
Red Marrow	0.12	0.10	0.12*
Thyroid	0.02	0.04	0.03
Bone Surface	0.03	0.03	0.03
Remainder	0.30	0.30	0.30
Totals	0.84	1.12	1.00

* The fact that the average of the male and female weighting factors do not exactly equal these values has no calculational significance.

Specifically, the risk factors for each organ in each gender were divided by the overall population risk implied by the ICRP-26 weighting factors. When this approach is used the weighting factors for the male and female do not sum to one because a female is more at risk than a male for the same exposure. The weighting factors are normalized so that the average for a population is one, as is done in ICRP-26 and 10 CFR 20.

Finally, there is one additional point to be made about the way the "remainder" organs are handled. (Recall that the five remainder organs receiving the highest dose are to be weighted and summed.) In order to perform a calculation that is conservative (that is, yields the highest assessed dose) we have chosen to make the list of remainder organs as complete as is reasonably possible. Basically any organ modeled in the reference phantom is tracked, even though some of these organs are not known to be susceptible to radiation-induced cancer. The list of remainder organs from which the five receiving the highest dose are selected is shown in Table 3.

2.3 The Photon Transport Computer Code

As noted previously, we used a Monte Carlo code to perform the beam and point source organ dose calculations and the surface flux calculations for this study. There are many advantages to the Monte Carlo technique. The basic physics of radiation transport required by Monte Carlo techniques is well understood, and it is much easier to

Table 3
Remainder Organs

Adrenals	Liver	Spleen
Arm Bones	Lower Rib Cage	Spine
Ascending Colon	Male Genitalia	Stomach
Brain	Middle Inner Chest	Thymus
Clavicles	Outer Trunk	Transverse Colon
Descending Colon	Pancreas	Upper Bladder
Gall Bladder	Pelvis	Upper Inner Chest
Head and Neck	Ribs	Upper Rib Cage
Heart	Scapulae	Uterus
Kidneys	Sigmoid Colon	Very Upper Torso
Leg Bones	Skull	
Legs	Small Intestine	

obtain satisfactory results for routine geometries by calculational methods compared to direct measurement with anthropomorphic phantoms. Calculational methods also inherently provide strong documentation. The necessary radiation transport software has been developed and has been extensively verified, and microcomputers are now available that are sufficiently fast to run these problems in a reasonable length of time. And, as described above, accurate mathematical models of humans are developed, published, and widely used within the radiation protection community.

The Monte Carlo radiation transport code selected for this study was MCNP (Monte Carlo Neutron-Photon).¹⁰ MCNP, developed at Los Alamos National Laboratory, is available from the Radiation Shielding Information Center (Oak Ridge, TN). The first version of MCNP was published in 1977, but the code has its roots in the earliest Monte Carlo neutron transport codes written at Los Alamos in the late 1950s and early 1960s. The code has been used by researchers throughout the world, is extensively documented, and has been used successfully to run tens-of-thousands of practical problems.

MCNP allows a user to specify a problem as a set of cells that fill up a model universe. These cells are defined by means of a set of surfaces and their intersections and unions. For these calculations the cells were the organ and tissue models within the anthropomorphic phantoms described in Section 2.2.1. Given a problem geometry, properties of that geometry, and a source description, the code can be used to model transport of photons through the model and tally various kinds of results. The code is capable of more than just basic transport simulation. It also has features that make problem set up, verification, and data analysis easier.

MCNP has approximately 28,000 lines of source code. After expansion by a post-processor (a part of the MCNP software), the code contains about 78,000 source lines occupying 5.3 megabytes of space. It was originally written to run on a Cray or other large computer, although it is now available for a variety of platforms—including the IBM PC—from the Radiation Shielding Information Center. We chose to port the code to a Macintosh IIx equipped with 8 megabytes of memory, a 100 megabyte hard disk drive, and a 33 MHz accelerator card. We wrote a post-processor code to extract the essential data from the MCNP output, thereby eliminating the need

for manual searches through the voluminous output (approximately 6 Mbytes per run). The post-processor code located certain information, manipulated it if necessary, and printed the results, including:

- basic "header" information (source type, direction, etc.)
- organ doses and organ dose errors
- the product of the organ dose and its gender-specific weighting factor
- the five highest remainder organs
- the product of the remainder organ doses and their gender-specific weighting factors
- the sum of all the doses
- energy and photon fluxes at specific locations on the phantoms' surfaces (corresponding to the angles and energies used for the organ dose calculations)
- the results of an error propagation analysis.

Appendices B and C are compilations of the summary sheets created by the post-processor.

We did not originally plan on implementing MCNP's graphics capabilities, but the potential advantages made themselves apparent early on. The method of defining geometries in MCNP is a bit obtuse, and it is difficult to be certain that the defined shape corresponds to one's mental image of it. Accordingly, we wrote subroutines that allow the Macintosh to emulate a set of graphics drivers (called the GKS library) that enabled it to drive a Tektronics terminal. The compiled and linked code ready to run on a Macintosh occupies 1.4 megabytes of disk space.

Part way into the study Los Alamos released Version 4 of MCNP (we had been using Version 3.b), which would run on a 386-based personal computer. (Version 4 also corrected some minor subroutine errors and added some extra functions not used in this study.) We obtained Version 4 and subsequently implemented it on 486-based personal computers. Extensive cross-checks and verifications assured us that our microcomputer MCNP codes matched all applicable benchmarks, and the PC and Macintosh versions were consistent with each other.

3

THE RESULTS OF THE EFFECTIVE DOSE EQUIVALENT CALCULATIONS

3.1 Overview of the EDE Calculations

Effective dose equivalent is a slowly varying function of photon energy. Accordingly, one need perform effective dose equivalent assessments on only a few energies to effectively map the results; other energies can be interpolated. For this study, three photon energies—0.08, 0.3, and 1.0 MeV—were used with each gender phantom to map the response for a given exposure geometry. (These energies adequately bound the photon energies encountered in a nuclear power facility.) For each phantom and for each energy, a series of geometries were calculated. First, beam sources from many three-dimensional angles of incidence were calculated. These were done at sufficient solid angle intervals so that effective dose equivalent and organ doses could be calculated by interpolation for any beam angle. Next, effective dose from point sources at various distances from the phantoms (ranging from contact to three meters) were calculated. Surface photon fluxes (both energy fluxes and simple photon fluence rates) were also calculated for some of the same beam angles and point source locations. These surface flux results were used to develop conversion factors and methodologies for estimating effective dose equivalent in various photon radiation fields. Surface flux values and the effective dose conversion methodologies will be published later as Volume II of this study.

3.2 Beam Source Results

We used a beam geometry for our first efforts to determine effective dose equivalent from external photon exposures. Beams, which irradiate uniformly across the height of the torso, were selected for a number of reasons. Beams are an easy geometry to understand and characterize. For a known energy, beam intensity can be

characterized by a single parameter, either photons/cm²-s or MeV/cm²-s. All finite sources behave as beam sources as the distance between the source and the receptor increases. Thus, if we understand beam sources we understand the limiting case for all other finite sources. Finally, the beam geometry is the most prevalent geometry reported in the literature, allowing us ample data for early checks on our calculations.

A standard polar-azimuthal angle system is used for naming the three-dimensional angles that describe the incident beam (see Figure 4). Polar angles run from 0° (beams directly overhead) to 180° (beams directly underfoot). Looking down on the torso from above, azimuthal angles run clockwise from 0° (beams incident on the front of the torso), to 180° (beams incident on the rear of the torso), and continuing around the torso to 360° (beams again incident on the front). Beams striking the torso from the front are termed *anterior-posterior* beams (abbreviated AP). Beams striking the torso from the rear are termed *posterior-anterior* beams (abbreviated PA). And beams striking the torso from the side are termed *lateral* beams (abbreviated LAT). These irradiation geometries are illustrated in Figure 5.

Calculations were done first using the following beam geometries:

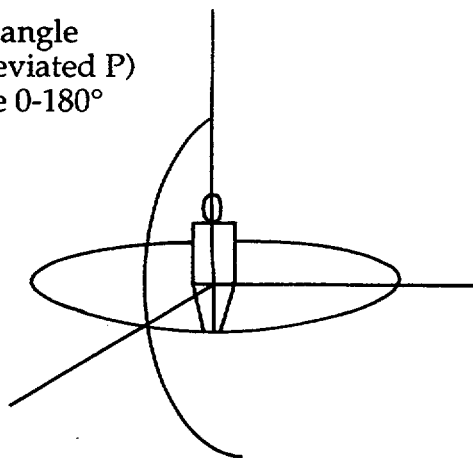
- Anterior-posterior beams incident directly on the front of the torso (using the nomenclature of Figure 4, P90-A0)
- Posterior-anterior beams incident directly on the rear of the torso (P90-A180)
- And two lateral exposures (P90-A90 and P90-A270).

To verify our calculational method, we compared our results to ICRP-51⁸. ICRP-51 presents calculational results for beam sources in the AP, PA, and LAT geometries and—being from an accepted international advisory group—represents an excellent benchmark.

The results of our calculations and their comparison with ICRP-51 are presented in Table 4 and Figure 6.* They indicate good agreement over the entire photon energy range. The largest difference is about 13% for the

PA exposure with 0.08 MeV photons. This difference results, in part, because we use gender-specific weighting factors and average the results, while the ICRP calculated effective dose equivalent using sex-averaged weighting factors on a single phantom. All other values agree within 10%, which is excellent considering different transport codes and slightly different phantoms were used. We conclude that this agreement provides verification of our methodology for beam geometries.

Polar angle
(abbreviated P)
Range 0-180°



Azimuthal angle
(abbreviated A).
Range 0-360°

Example:

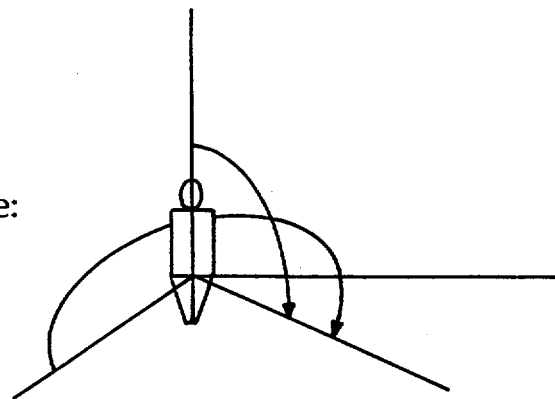


Figure 4. Nomenclature used to describe the beam angle of incidence

* Generally, the rem dose unit is used in this report rather than the sievert, because that is the unit used in 10 CFR 20 and the unit commonly used by the utility industry. Sieverts are sometimes used in figures, however, when making comparisons to literature results that use that unit. A sievert equals 100 rem.

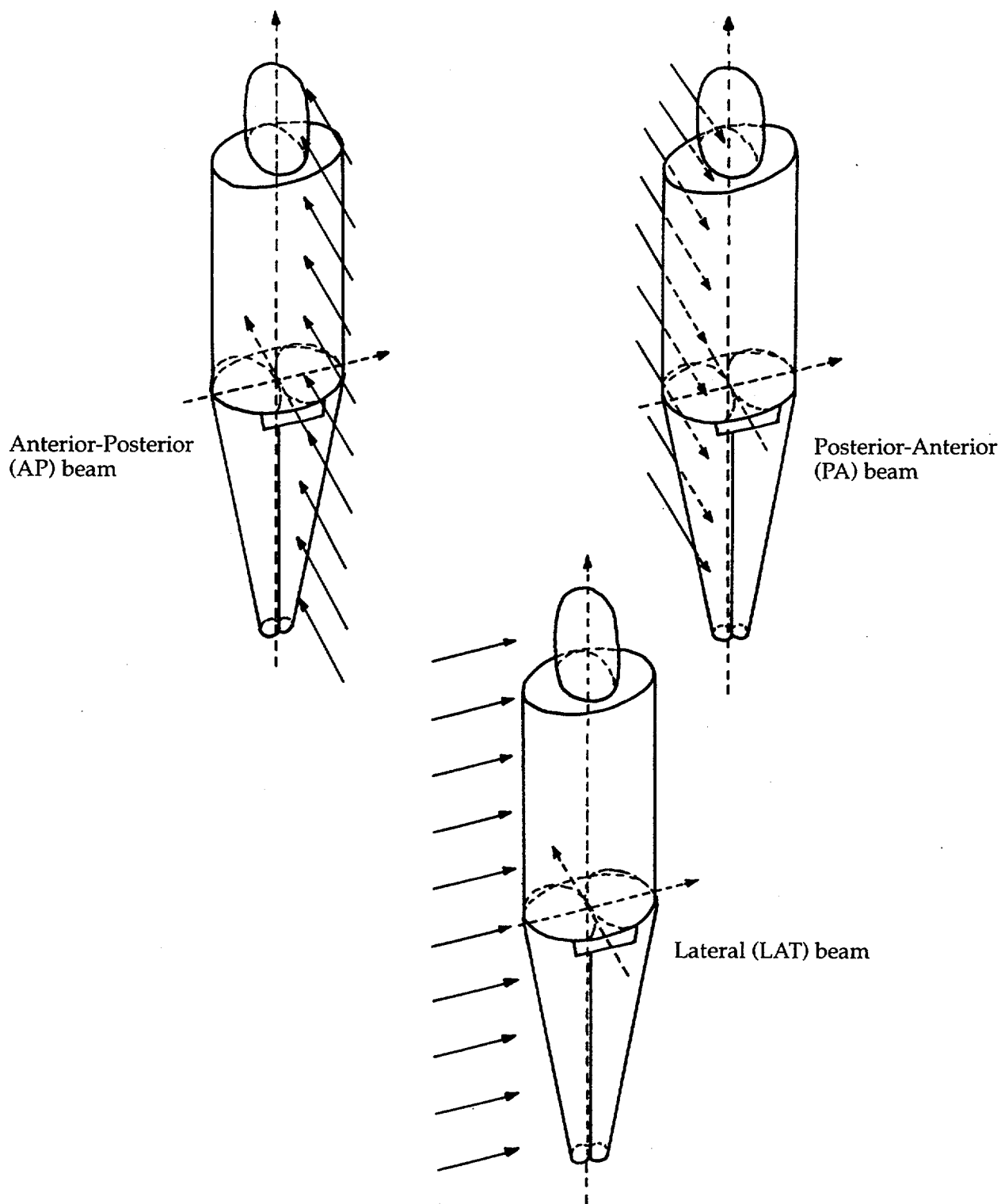


Figure 5. Phantom irradiation geometries

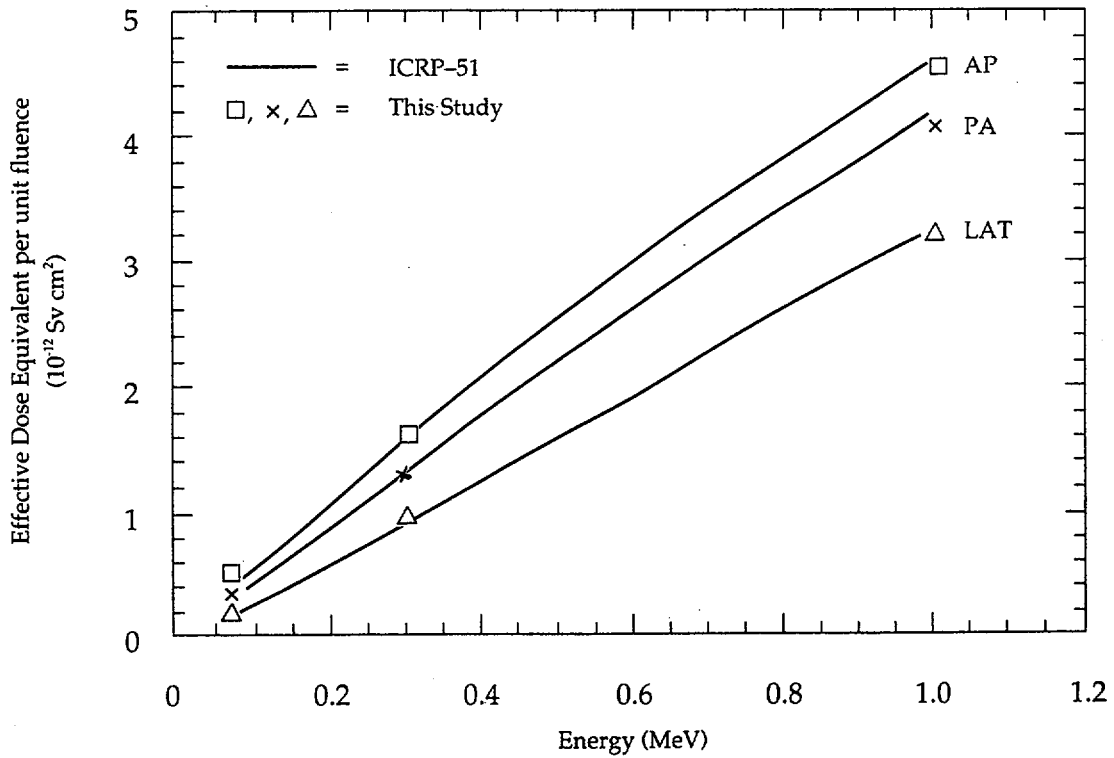


Figure 6. Effective dose equivalent vs. photon energy for beam geometries

Table 4
Effective Dose Equivalent Comparison of This Study With ICRP-51

Geometry	Photon Energy (MeV)	ICRP-51 (10^{-12} Sv-cm^2)	This Study* (10^{-12} Sv-cm^2)
AP	0.08	0.451	0.482 ± 0.009
AP	0.30	1.560	1.559 ± 0.026
AP	1.00	4.600	4.555 ± 0.077
PA	0.08	0.344	0.395 ± 0.007
PA	0.30	1.300	1.297 ± 0.023
PA	1.00	4.180	4.048 ± 0.070
LAT	0.08	0.212	0.229 ± 0.005
LAT	0.30	0.891	0.895 ± 0.014
LAT	1.00	3.240	3.215 ± 0.056

* Average of male and female

After confirming our methodology, phantoms, and calculational technique, we mapped the effect of beam direction through all three-dimensional angles. Well over 100 beam angles were calculated. This provided sufficient detail to allow simple interpolation through any two adjacent angles, such that effective dose equivalent errors would be equal to or less than the errors inherent in the calculations themselves. One page sheets summarizing the MCNP calculations for each energy, gender, and beam angle are presented in Appendix B. These sheets list calculated doses for each organ, estimated error for each calculated organ dose, effective dose equivalent based on estimated organ doses, and calculated overall error in the H_E calculation.

Figures 7 and 8 summarize the results for radiation beams traversing the principal azimuthal and polar great circles. In order to make these figures easier to interpret, we have added small human icons to the top of each one. The location and orientation of these human icons on the figure is important. Their location corresponds to the azimuthal or polar angles shown on the figure, and their orientation gives the reader a quick reminder of the way the radiation beam is striking the phantom. Figure 7 shows the variation of H_E as a function of photon energy, gender, and azimuthal angle, with the polar angle fixed at 90° (normal to the body's major axis). Figure 8 shows the variation of H_E as a function of photon energy, gender, and polar angle, with the azimuthal angle fixed at 0° – 180° (normal to the body's major axis).

These plots are only a small sampling of the data collected from the beam studies. Figures similar to those above, for example, could be drawn for many other great circles covering the full spectrum of azimuthal and polar angles. Tables 5 through 7 present the data for all of the polar and azimuthal angles that were calculated. The data can be plotted in a variety of other forms. Figures 9 and 10, for example, combine three-dimensional surface projection plots and contour plots. They show effective dose equivalent versus polar and azimuthal angle for a 1.0 MeV photon beam incident upon a male and a female. Although quantitative data are difficult to extract from such figures, they do illustrate quite clearly how H_E varies with gender for all beam locations. Projection and contour plots for the other photon energies are included in Attachment 1. (Attachment 1 is located immediately following the main text; it is not on the computer disk.)

Several important results are immediately apparent from the beam data. Beams striking the torso normal to the body's major axis (AP or PA beams) produce the largest H_E . In all cases, H_E is higher for the beams striking the front of the torso (AP) than it is for beams striking the rear of the torso (PA). Effective dose equivalent falls dramatically as one departs from the AP or PA orientation. Dosimeter badge response also falls, but often effective dose equivalent falls faster.¹¹ Therefore, dosimeters would not under predict H_E regardless of the incident photon angle. Although concern has been expressed in the literature about underfoot and overhead sources, the actual effective dose equivalent drops markedly for these geometries.

For equivalent energy fluxes, lower energy photons always produce lower effective dose equivalents. This arises primarily from shielding of the deeper organs and the part of the torso away from the beam by parts of the body proximate to the beam. This is contrary to flux-to-dose relationships published by ANSI¹² and used throughout the nuclear industry (see Figure 11). Because the ANSI Standard is based on maximum dose 1-cm deep in tissue, there appears to be a minimum in the flux-to-dose conversion at about 80 keV, and then the conversion factor increases. Flux-to-dose conversions based on effective dose equivalent concepts decrease monotonically with energy at rates that increase with decreasing energy. Thus, the ANSI standard greatly over predicts dose for low energy photons.

Perhaps most important, this report demonstrates that dose assessment methodologies for external photons can be based on fully developed anthropomorphic phantoms rather than on the simple slabs, cylinders, or spheres as is the current practice. This should help end overly conservative exposure estimates, and open the door to determining radiation exposures that realistically estimate the risk of radiation injury.

3.3 Point Source Results

After completing the beam geometry study, doses from point sources were investigated. This geometry is the most difficult to characterize because effective dose equivalent is a function not only of source intensity, but also of distance from the phantom. However, the reward for complete characterization is large. Once H_E can be predicted for a point anywhere external to the phantom, then dose from all other simple sources can be calculated

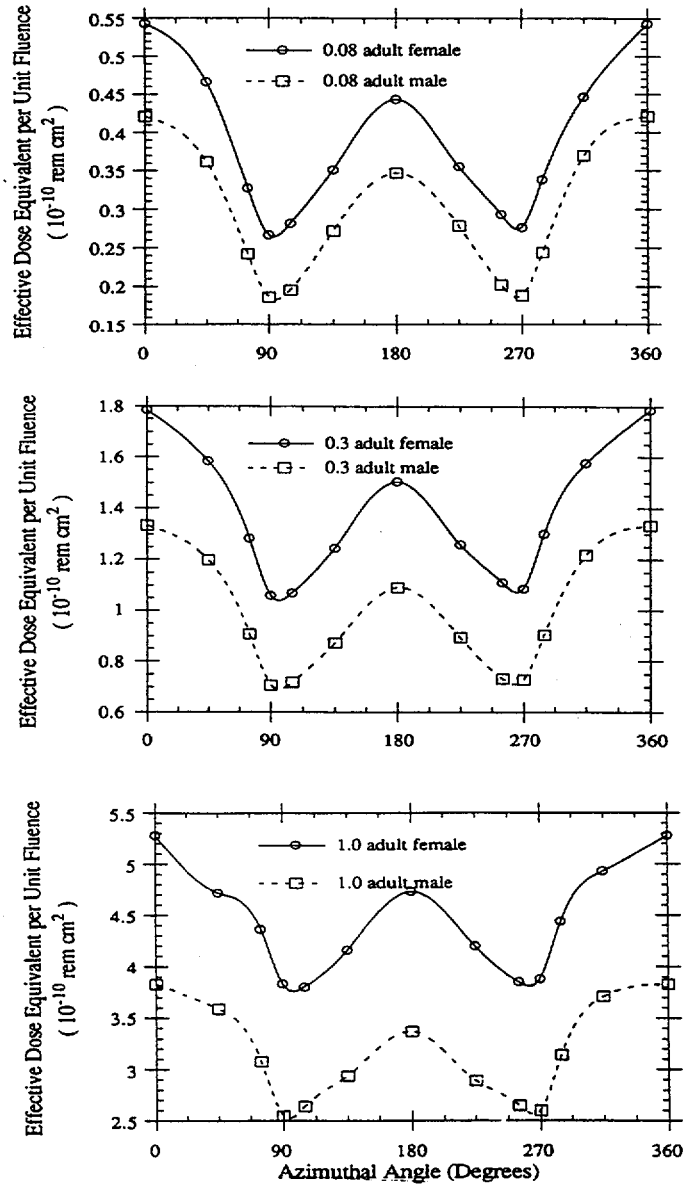
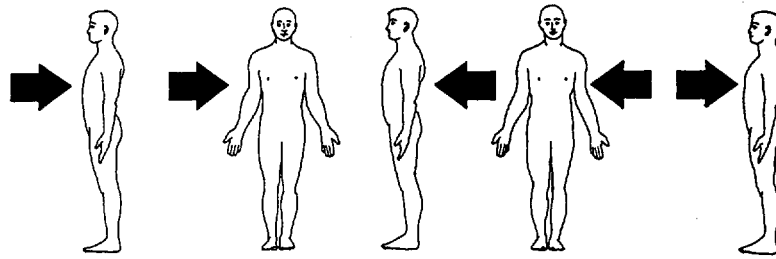


Figure 7. Effective dose equivalent vs. azimuthal angle

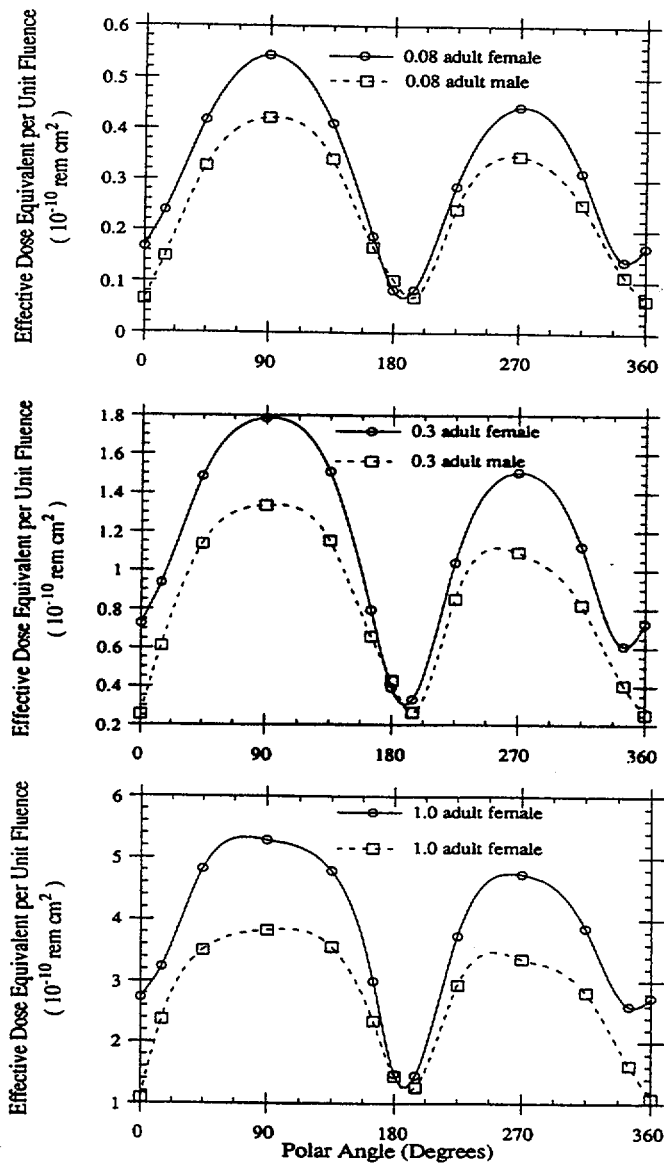
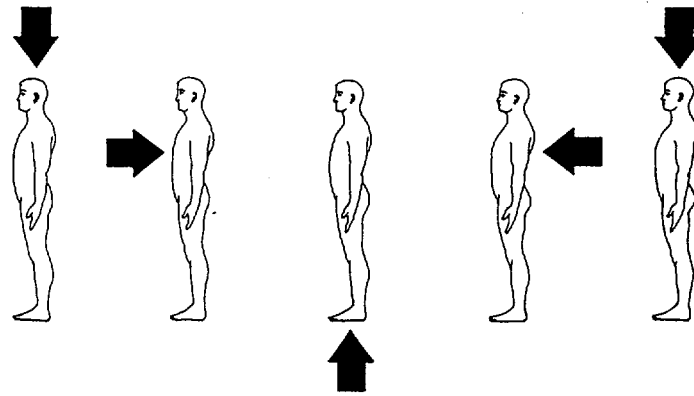


Figure 8. Effective dose equivalent vs. polar angle

Table 5
Effective Dose Equivalent for 0.08 MeV Photon Beams as a Function of Polar and Azimuthal Angle
 (units = E-10 rem-sq cm)

Adult Female

Polar Angle	0°	15°	45°	90°	135°	165°	180°
Azimuthal Angle							
0°	0.167	0.238	0.417	0.543	0.410	0.188	0.083
45°	0.167	0.221	0.349	0.466	0.336	0.165	0.083
75°	0.167	0.186	0.275	0.327	0.240	0.130	0.083
90°	0.167	0.168	0.232	0.266	0.190	0.103	0.083
105°	0.167	0.144	0.221	0.281	0.182	0.080	0.083
135°	0.167	0.135	0.258	0.351	0.220	0.071	0.083
180°	0.167	0.141	0.314	0.443	0.286	0.083	0.083
225°	0.167	0.135	0.263	0.355	0.241	0.073	0.083
255°	0.167	0.145	0.223	0.293	0.192	0.084	0.083
270°	0.167	0.168	0.241	0.276	0.198	0.106	0.083
285°	0.167	0.190	0.283	0.338	0.235	0.133	0.083
315°	0.167	0.217	0.355	0.446	0.335	0.166	0.083
360°	0.167	0.238	0.417	0.543	0.410	0.188	0.083

Adult Male

Polar Angle	0°	15°	45°	90°	135°	165°	180°
Azimuthal Angle							
0°	0.065	0.148	0.327	0.421	0.340	0.167	0.103
45°	0.065	0.118	0.270	0.362	0.276	0.146	0.103
75°	0.065	0.085	0.177	0.242	0.187	0.117	0.103
90°	0.065	0.076	0.139	0.186	0.116	0.082	0.103
105°	0.065	0.079	0.147	0.195	0.115	0.038	0.103
135°	0.065	0.092	0.204	0.272	0.182	0.049	0.103
180°	0.065	0.111	0.252	0.347	0.241	0.069	0.103
225°	0.065	0.095	0.208	0.278	0.189	0.051	0.103
255°	0.065	0.080	0.147	0.202	0.123	0.039	0.103
270°	0.065	0.077	0.145	0.188	0.119	0.088	0.103
285°	0.065	0.086	0.184	0.244	0.184	0.169	0.103
315°	0.065	0.119	0.271	0.370	0.273	0.149	0.103
360°	0.065	0.148	0.327	0.421	0.340	0.167	0.103

Table 6
Effective Dose Equivalent for 0.3 MeV Photon Beams as a Function of Polar and Azimuthal Angle
 (units = E-10 rem-sq cm)

Adult Female

Polar Angle	0°	15°	45°	90°	135°	165°	180°
Azimuthal Angle							
0°	0.727	0.936	1.483	1.785	1.507	0.796	0.392
45°	0.727	0.872	1.341	1.584	1.276	0.704	0.392
75°	0.727	0.791	1.087	1.283	0.979	0.559	0.392
90°	0.727	0.706	0.931	1.059	0.796	0.448	0.392
105°	0.727	0.593	0.888	1.068	0.749	0.341	0.392
135°	0.727	0.542	0.949	1.245	0.863	0.284	0.392
180°	0.727	0.608	1.122	1.503	1.038	0.329	0.392
225°	0.727	0.536	0.976	1.259	0.900	0.291	0.392
255°	0.727	0.590	0.880	1.110	0.784	0.349	0.392
270°	0.727	0.706	0.950	1.086	0.830	0.454	0.392
285°	0.727	0.778	1.112	1.301	0.968	0.568	0.392
315°	0.727	0.875	1.318	1.575	1.290	0.693	0.392
360°	0.727	0.936	1.483	1.785	1.507	0.796	0.392

Adult Male

Polar Angle	0°	15°	45°	90°	135°	165°	180°
Azimuthal Angle							
0°	0.255	0.610	1.137	1.333	1.155	0.659	0.429
45°	0.255	0.505	1.005	1.199	0.999	0.576	0.429
75°	0.255	0.344	0.715	0.908	0.761	0.483	0.429
90°	0.255	0.297	0.547	0.707	0.499	0.353	0.429
105°	0.255	0.286	0.542	0.717	0.467	0.151	0.429
135°	0.255	0.337	0.691	0.872	0.623	0.183	0.429
180°	0.255	0.405	0.821	1.092	0.850	0.264	0.429
225°	0.255	0.336	0.708	0.895	0.654	0.198	0.429
255°	0.255	0.290	0.555	0.732	0.486	0.162	0.429
270°	0.255	0.291	0.579	0.728	0.503	0.365	0.429
285°	0.255	0.351	0.733	0.905	0.752	0.466	0.429
315°	0.255	0.488	1.003	1.219	0.977	0.583	0.429
360°	0.255	0.610	1.137	1.333	1.155	0.659	0.429

Table 7
Effective Dose Equivalent for 1.00 MeV Photon Beams as a Function of Polar and Azimuthal Angle
 (units = E-10 rem-sq cm)

Adult Female

Polar Angle	0°	15°	45°	90°	135°	165°	180°
Azimuthal Angle							
0°	2.730	3.240	4.820	5.280	4.780	3.000	1.480
45°	2.730	3.090	4.320	4.720	4.350	2.730	1.480
75°	2.730	2.870	3.870	4.360	3.580	2.110	1.480
90°	2.730	2.690	3.450	3.830	3.140	1.720	1.480
105°	2.730	2.310	3.340	3.800	2.860	1.380	1.480
135°	2.730	2.240	3.480	4.160	3.280	1.310	1.480
180°	2.730	2.590	3.860	4.730	3.740	1.450	1.480
225°	2.730	2.220	3.590	4.200	3.320	1.360	1.480
255°	2.730	2.330	3.280	3.850	3.010	1.400	1.480
270°	2.730	2.670	3.470	3.880	3.260	1.760	1.480
285°	2.730	2.890	3.940	4.440	3.550	2.130	1.480
315°	2.730	3.110	4.410	4.930	4.270	2.680	1.480
360°	2.730	3.240	4.820	5.280	4.780	3.000	1.480

Adult Male

Polar Angle	0°	15°	45°	90°	135°	165°	180°
Azimuthal Angle							
0°	1.090	2.370	3.510	3.830	3.560	2.350	1.440
45°	1.090	2.070	3.280	3.590	3.200	2.120	1.440
75°	1.090	1.520	2.680	3.080	2.710	1.680	1.440
90°	1.090	1.270	2.260	2.550	2.090	1.440	1.440
105°	1.090	1.190	2.140	2.640	2.000	0.810	1.440
135°	1.090	1.390	2.470	2.940	2.410	0.870	1.440
180°	1.090	1.620	2.820	3.370	2.940	1.260	1.440
225°	1.090	1.370	2.530	2.890	2.410	0.940	1.440
255°	1.090	1.200	2.140	2.650	2.050	0.850	1.440
270°	1.090	1.250	2.220	2.600	2.070	1.420	1.440
285°	1.090	1.560	2.750	3.140	2.740	1.730	1.440
315°	1.090	2.060	3.320	3.710	3.240	2.070	1.440
360°	1.090	2.370	3.510	3.830	3.560	2.350	1.440

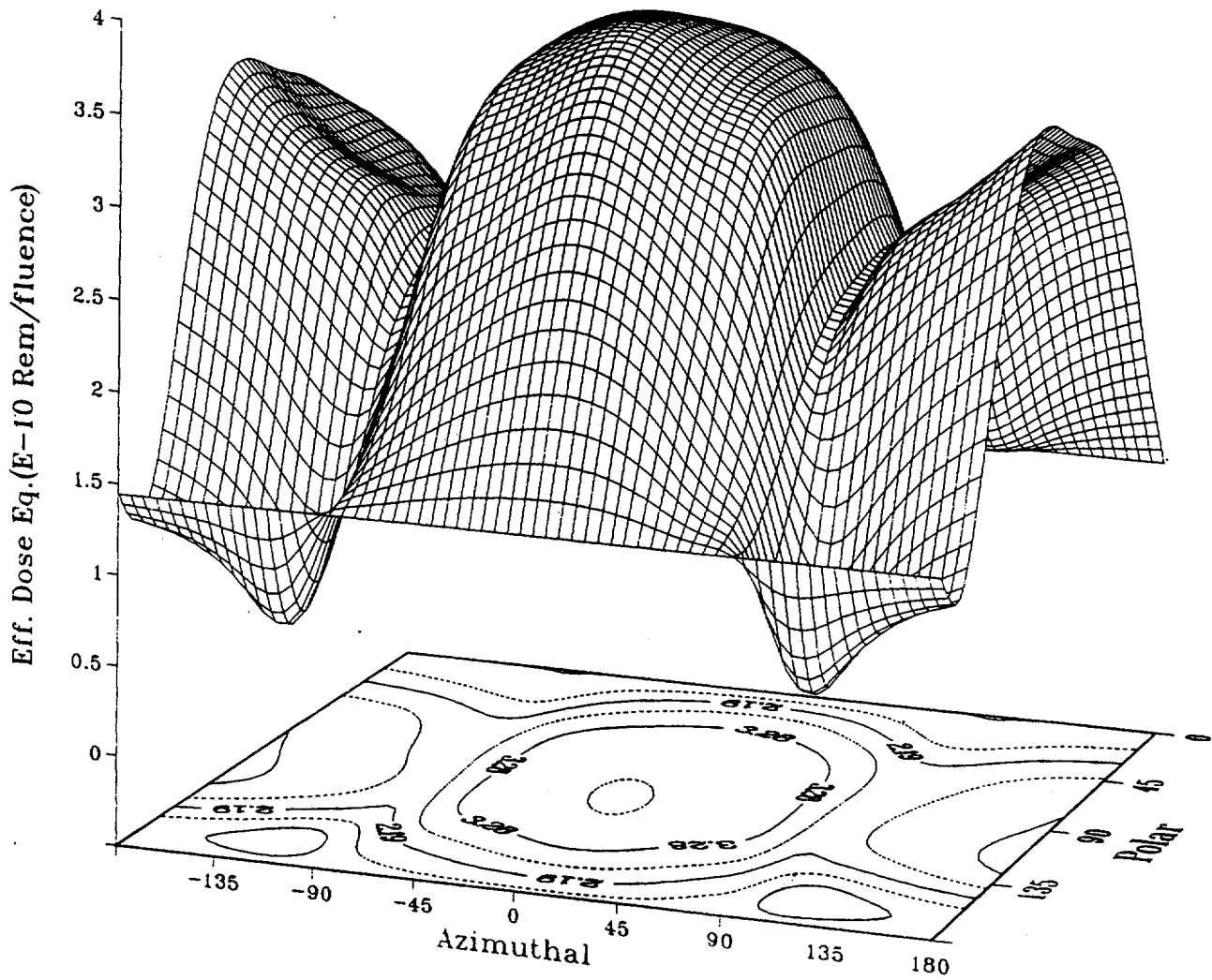


Figure 9. Surface and contour plots of effective dose equivalent for a male for 1.0 MeV photon beams

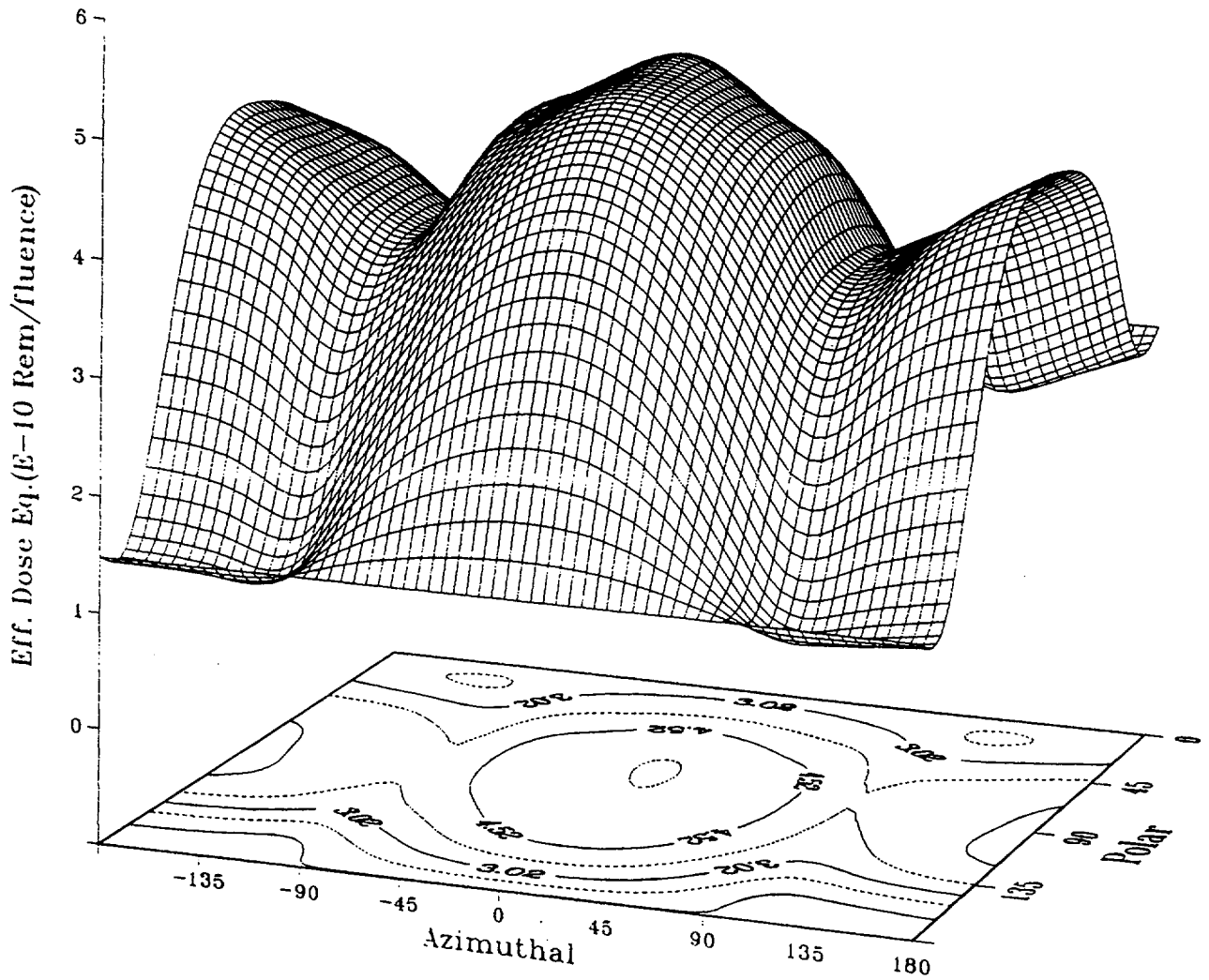


Figure 10. Surface and contour plots of effective dose equivalent for a female for 1.0 MeV photon beams

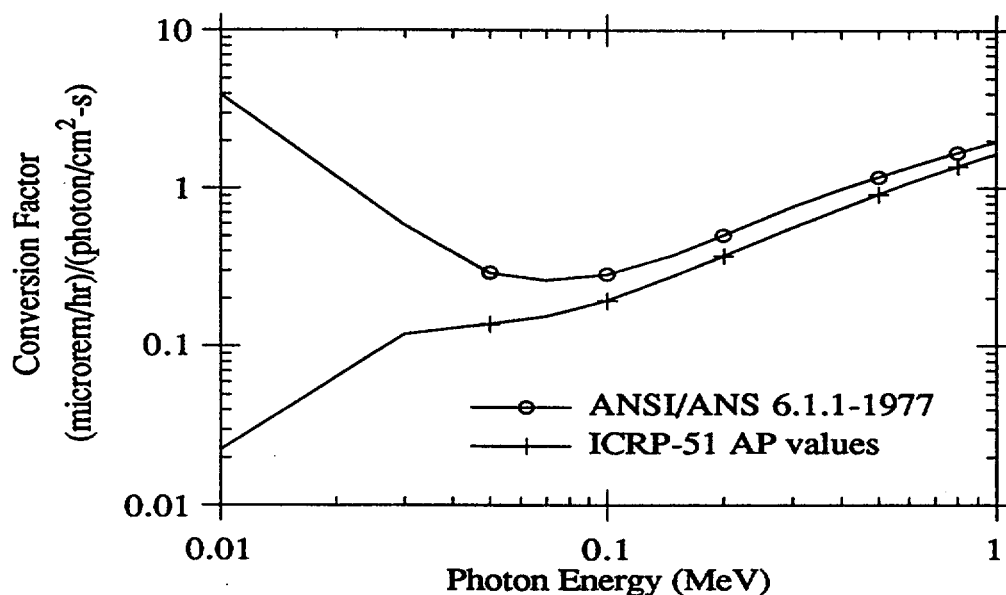


Figure 11. Flux-to-dose conversion factors

directly. A line source, for example, would be computationally divided into pieces small enough to be approximated by point sources, and the effects of all the pieces summed to calculate the overall dose from the line. Plane and disk sources can be handled in much the same way.

Hundreds of point sources were run at photon energies of 0.08, 0.3, and 1.0 MeV. We started with points in contact with the phantom torso, and moved the sources outward to three meters from the coordinate system origin. A diagram of the coordinate system used in MCNP to describe the phantom and the surrounding space is shown in Figure 12. The phantom is centered on the z-axis facing the negative y-direction. Thus, points in space with negative y-coordinate values are in front of the phantom, while those with positive y-coordinate values are to the rear. Complete tables of the calculated H_E versus gender, photon energy, and source position are presented in Appendix C.

3.3.1 Results With Point Sources in Contact With the Torso

Because the phantom torso is mathematically described by an equation for a right elliptical cylinder, the surface can be flattened into two dimensions without distortion. The reader should imagine the torso surface being cut along the right side, then folded open and flattened out. (The process would be analogous to cutting a can down its side, bending the can open, and then flattening it.) With the torso so flattened it is easy to visualize how dose versus location on the torso can be mapped in two dimensions. Tables 8 through 10 list effective dose equivalent as a function of gender, photon energy, and position of the source on the torso. Location on the torso is expressed as height above the data plane at the bottom of the torso (the plane at $z = 0$) and distance around the torso (starting at the right side, continuing across the front to the left side, and continuing around the rear and

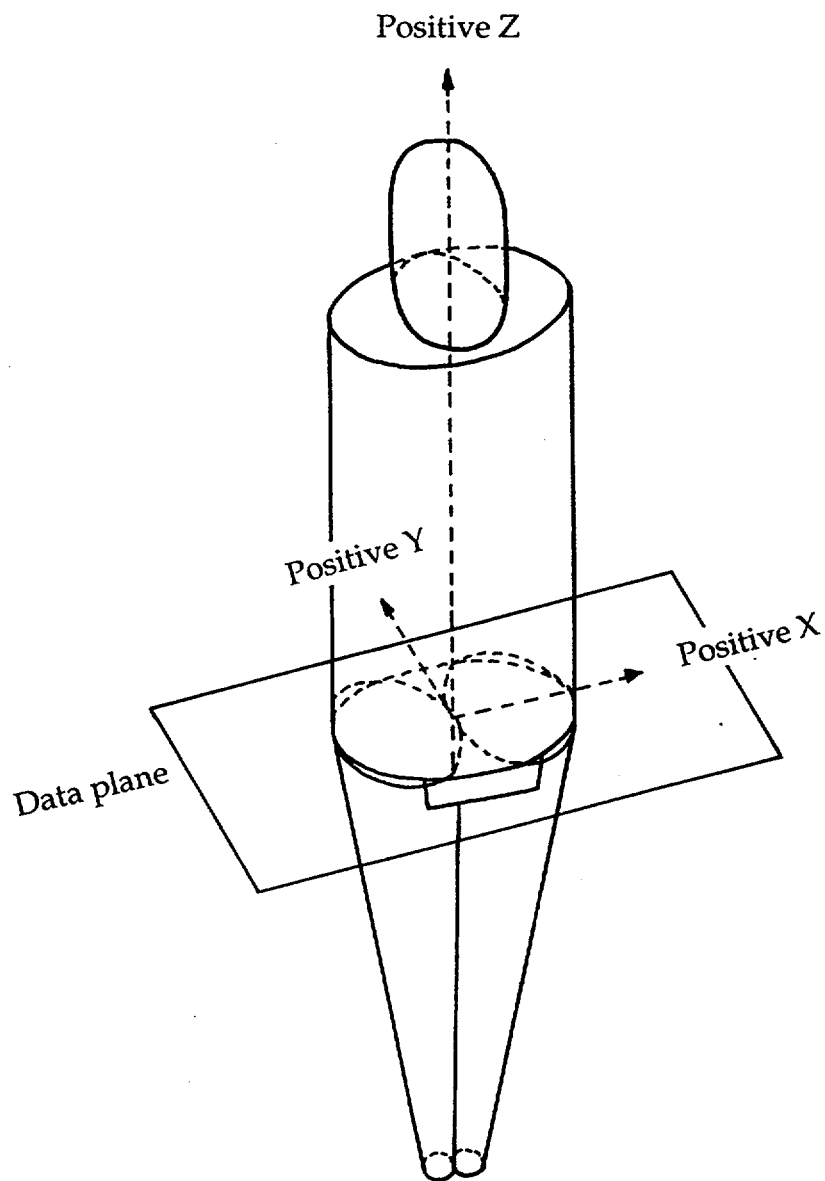


Figure 12. Schematic of the phantom coordinate system

terminating back at the right side). A contour maps for males and females showing H_E as a function of the position on the body of a point source radiating 1.0 MeV photons is shown in Figure 13. Similar contour maps for 0.08 and 0.3 MeV photons are presented in Attachment 1. Complete results for point sources in contact with the phantom are in Appendix C1.

For all photon energies, the highest effective dose equivalents for point sources in contact with the female torso occurs when the point source is on the front of the torso near the sternum. For males it occurs when the source is on the front of the torso near the gonads. For all photon energies, effective dose equivalent from a point source on the male gonads is higher than the effective dose equivalent from an identical source on the sternum of the female. However, for all other point source locations, the female has a higher effective dose equivalent per unit exposure than the male.

3.3.2 Results With Point Sources Away From the Torso

Doses from point sources three meters or more away from the phantom can be predicted using beam geometry results. As point sources are moved further away from the phantom, photons from these sources arrive ever more parallel, asymptotically approaching beam geometry. The intensity of point source far from the phantom is proportional to the square of the distance between the source and the phantom:

$$\begin{aligned} \text{intensity [photons/cm}^2\text{]} \\ = \text{photons emitted} / 4 \pi \text{ distance}^2 \end{aligned} \quad (\text{Eq. 9})$$

Consider the following example. Table 6 shows that a beam source of 0.3 MeV photons striking a female phantom at a polar angle of 45° and an azimuthal angle of 0° produces an effective dose equivalent of 1.48×10^{-10} rem per photon per cm^2 . For a 0.3 MeV point source located above and to the front of the female phantom 300 cm from the origin (i.e., at $x = 0.0$ cm, $y = -212.1$ cm, $z = 212.1$ cm) the calculated dose is 1.70×10^{-16} rem per photon emitted (see Appendix C3, page 3). When using Equation 9, what distance should be used in the formula? Should it be the closest distance to the phantom (212 cm)? Or should it be the distance from the center of the coordinate system (300 cm)? Using the geometric mean

of these two distances generally yields good agreement with the dose calculated by MCNP. In this example, the geometric mean is roughly the square root of the product of 212 and 300, or 252 cm. The predicted dose from the source is:

$$\begin{aligned} 1.48 \times 10^{-10} \text{ rem/photon/cm}^2 &= (4 \times 3.14 \times 252^2) \\ &= 1.86 \times 10^{-16} \text{ rem/photon} \end{aligned}$$

which is a good approximation to the calculated value of $1.70 \pm 0.03 \times 10^{-16}$. As the point source distance increases, the difference in distance between the closest location on the torso and the center of the coordinate system becomes a small fraction of the overall distance, and has little influence on the calculation. For point sources farther than three meters from the surface of the phantom, Equation 9 should calculate effective dose equivalent with an error less than 10%.

Source points located between contact and three meters are quite interesting to characterize. (The results of the MCNP calculations for point sources at contact, at one meter, and at three meters are in Appendices C1, C2, and C3 respectively.) Figure 14 shows three-dimensional projections of H_E versus point source location for a female exposed to a 1.0 MeV point source. The source is at a constant height—6, 41, or 61 cm—above the plane of the coordinate system (the plane that divides the torso and the legs of the phantom).^{*} Figure 15 shows a similar plot for males. The same data shown as contour plots are presented in Figures 16 and 17. (Projection and contour plots for the other photon energies are presented in Attachment 1. Summary sheets of the MCNP runs for the data points used in all these figures are presented in Appendix C4.)

There is considerable structure to this spatial region as the point sources move from contact with the body, and the doses asymptotically approach those predicted by beam geometry. Though the structure of the data plots appear complicated, the features are generally understood. By carefully considering the location and geometry of the radiation sources, the anatomical features of the phantom, and the relative weighting factors of the organs involved, the three-dimensional structures of the plots can be explained. Though the photon interactions with the body are complex, organ doses and effective dose equivalents can be readily calculated.

* Point sources 21 cm above the data plane were also calculated. These values were not plotted because they were very close to the values at 6 cm above the plane.

Table 8
Effective Dose Equivalent as a Function of Point Source Location on the Torso
(0.08 MeV Photons, units = rem per photon x E-15)

Adult Female

Distance From "Cut" (cm)*	Location on the Torso	Height Above Data Plane (cm)**			
		6	21	41	61
0.00	right side	1.56	2.49	2.76	2.10
5.15		2.54	4.58	5.93	5.44
15.03		5.35	8.89	10.88	11.74
25.30	front	9.19	9.60	11.48	15.21
35.56		5.88	7.95	12.28	11.65
45.44		2.75	4.08	6.76	5.40
50.59	left side	1.56	2.36	3.45	2.09
55.74		2.54	3.42	5.53	2.94
65.62		4.57	6.62	9.45	4.52
75.89	back	5.20	8.96	10.39	5.12
86.15		4.23	6.82	7.53	4.51
96.03		2.28	3.52	3.91	2.99
101.18	right side	1.56	2.49	2.76	2.10

Adult Male

Distance From "Cut" (cm)*	Location on the Torso	Height Above Data Plane (cm)**			
		6	21	41	61
0.00	right side	1.15	1.72	2.22	1.50
5.15		1.81	2.85	3.32	2.18
15.03		5.72	5.68	5.70	4.29
25.30	front	14.29	5.36	6.98	9.62
35.56		6.15	4.61	7.07	4.22
45.44		2.08	2.46	4.17	2.15
50.59	left side	1.15	1.59	2.90	1.48
55.74		1.74	2.29	5.07	2.50
65.62		2.93	4.19	8.81	3.87
75.89	back	3.01	5.91	9.86	4.63
86.15		2.49	4.33	6.80	3.85
96.03		1.45	2.38	3.43	2.53
101.18	right side	1.15	1.72	2.22	1.50

* The distance from the simulated "cut" along the right side of the torso (see text).

** The plane where the bottom of the torso meets the top of the legs (see Figure 12).

Table 9
Effective Dose Equivalent as a Function of Point Source Location on the Torso
(0.03 MeV Photons, units = rem per photon x E-15)

Adult Female

Distance From "Cut" (cm)*	Location on the Torso	Height Above Data Plane (cm)**			
		6	21	41	61
0.00	right side	6.96	10.77	12.52	9.42
5.15		9.77	17.27	23.13	20.95
15.03		19.18	31.77	40.13	43.83
25.30	front	32.21	19.14	42.85	56.34
35.56		20.40	28.53	45.12	43.62
45.44		10.94	16.22	26.01	20.89
50.59	left side	6.96	10.33	15.15	9.50
55.74		9.69	13.33	20.93	10.88
65.62		16.22	23.08	34.04	15.51
75.89	back	18.19	29.04	36.27	16.28
86.15		14.68	23.59	27.19	15.35
96.03		8.80	13.68	15.35	10.87
101.18	right side	6.96	10.77	12.52	9.42

Adult Male

Distance From "Cut" (cm)*	Location on the Torso	Height Above Data Plane (cm)**			
		6	21	41	61
0.00	right side	5.04	7.13	9.21	5.87
5.15		7.48	10.58	12.27	7.75
15.03		22.16	19.97	19.76	14.62
25.30	front	52.04	33.35	24.15	33.94
35.56		22.93	16.62	24.46	14.53
45.44		8.30	9.41	15.03	7.65
50.59	left side	5.04	6.65	11.78	5.87
55.74		6.64	8.63	18.34	8.44
65.62		10.29	13.71	30.33	12.21
75.89	back	10.81	17.80	33.04	13.44
86.15		8.60	14.18	23.49	12.04
96.03		5.63	8.84	12.69	8.39
101.18	right side	5.04	7.13	9.21	5.87

* The distance from the simulated "cut" along the right side of the torso (see text).

** The plane where the bottom of the torso meets the top of the legs (see Figure 12).

Table 10
Effective Dose Equivalent as a Function of Point Source Location on the Torso
(1.0 MeV Photons, units = rem per photon x E-15)

Adult Female

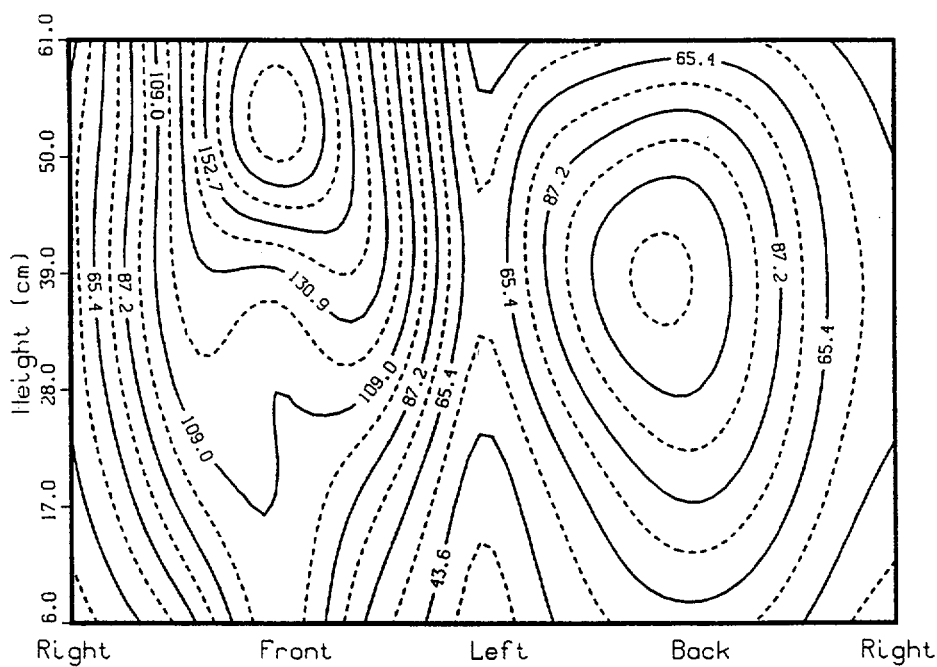
Distance From "Cut" (cm)*	Location on the Torso	Height Above Data Plane (cm)**			
		6	21	41	61
0.00	right side	26.43	41.71	49.49	37.82
5.15		36.75	60.29	78.24	70.07
15.03		64.17	103.50	129.80	140.40
25.30	front	103.90	109.20	137.80	179.00
35.56		68.29	93.64	144.50	140.40
45.44		38.91	57.06	87.24	70.04
50.59	left side	26.43	40.11	57.98	37.88
55.74		35.24	48.95	73.77	41.15
65.62		53.59	77.90	112.70	53.52
75.89	back	60.71	95.33	120.10	57.57
86.15		51.06	78.52	91.57	53.00
96.03		32.10	49.34	59.39	40.90
101.18	right side	26.43	41.71	49.49	37.82

Adult Male

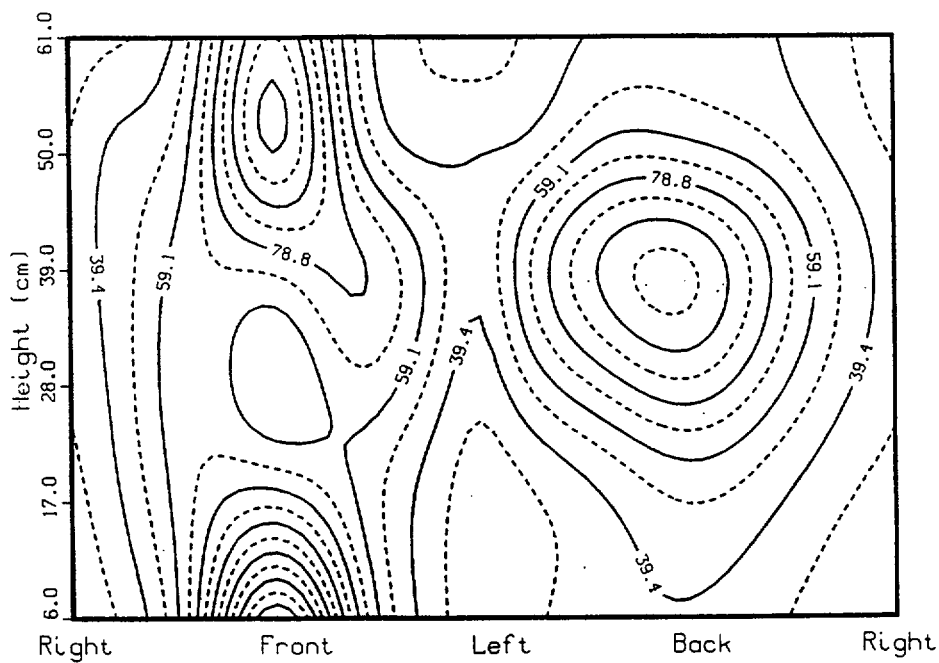
Distance From "Cut" (cm)*	Location on the Torso	Height Above Data Plane (cm)**			
		6	21	41	61
0.00	right side	20.83	27.82	34.26	22.56
5.15		29.11	38.66	42.56	27.64
15.03		75.75	67.22	65.02	48.91
25.30	front	168.50	65.31	79.20	109.10
35.56		77.36	57.16	79.38	48.92
45.44		31.56	34.61	51.53	27.52
50.59	left side	20.83	26.27	42.95	22.46
55.74		25.82	31.94	62.35	29.98
65.62		36.17	47.16	98.42	40.92
75.89	back	38.40	59.77	106.40	45.40
86.15		31.57	48.28	77.05	40.38
96.03		22.53	32.52	44.23	29.68
101.18	right side	20.83	27.82	34.26	22.56

* The distance from the simulated "cut" along the right side of the torso (see text).

** The plane where the bottom of the torso meets the top of the legs (see Figure 12).



Female



Male

Figure 13. Contour plots of H_E for 1.0 MeV point sources in contact with the body (units = 10⁻¹⁵ rem/photon emitted)

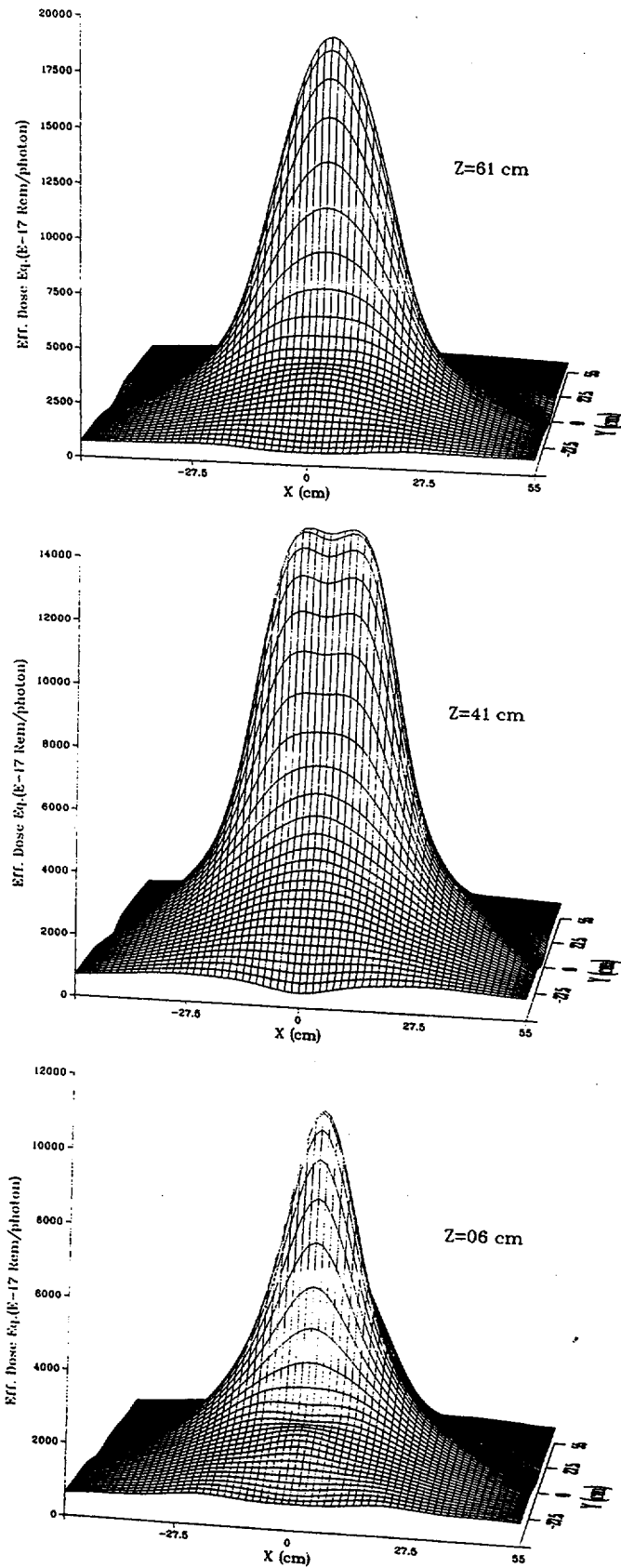


Figure 14. Surface plots of H_E for a female vs. source location for a 1.0 MeV point source

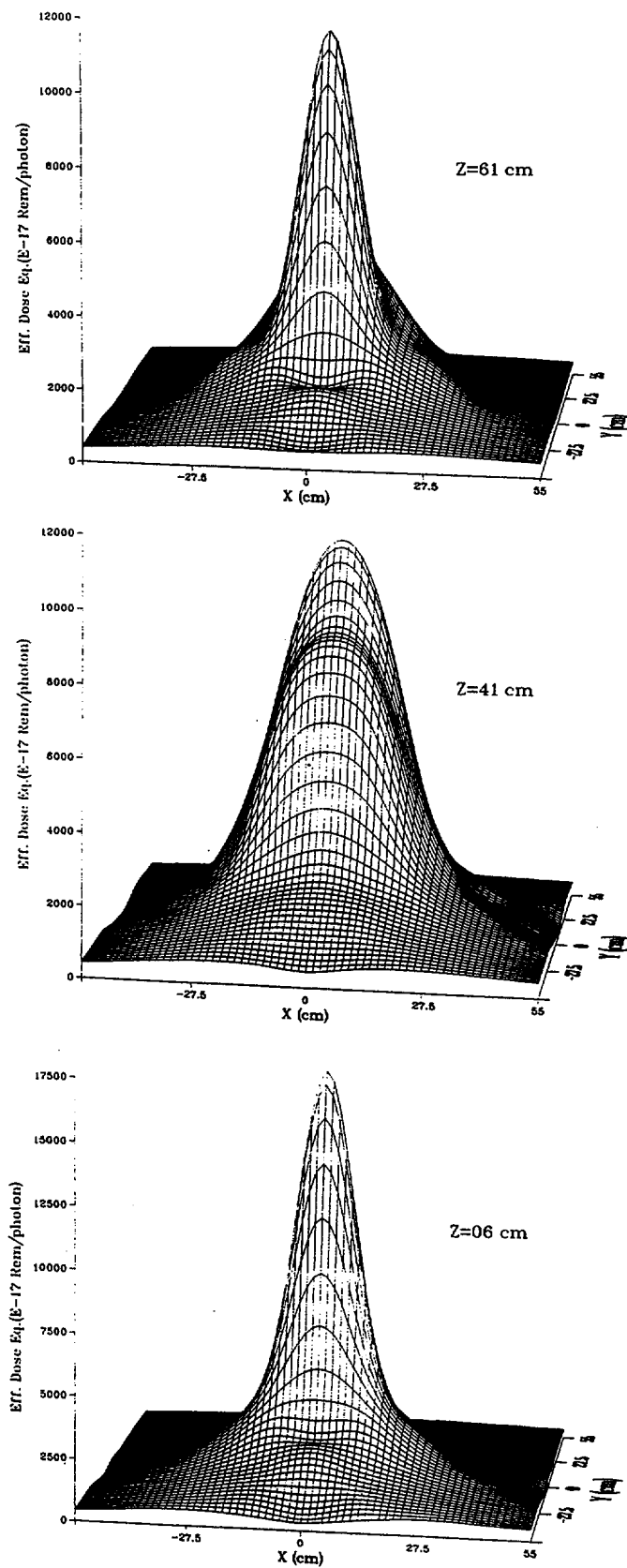


Figure 15. Surface plots of H_E for a male vs. source location for a 1.0 MeV point source

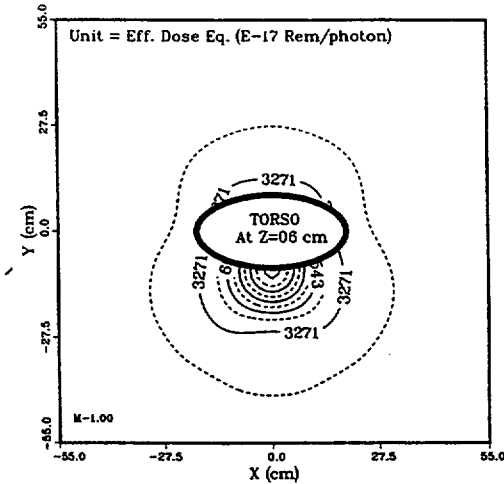
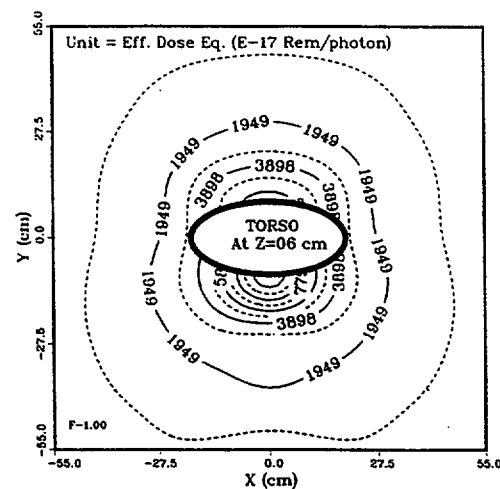
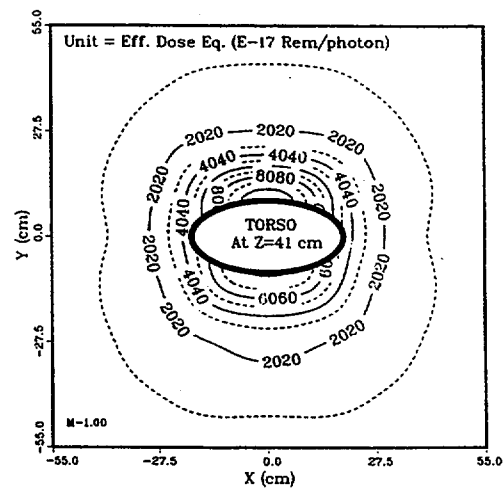
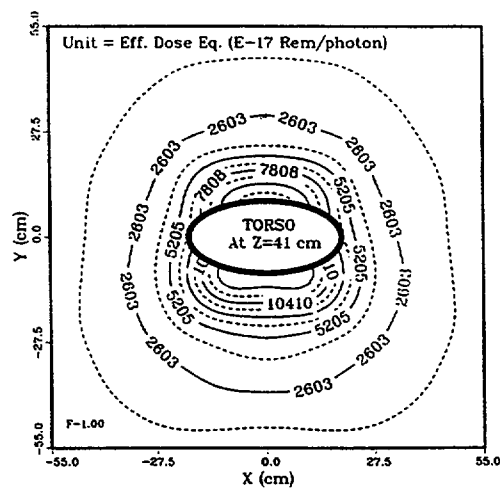
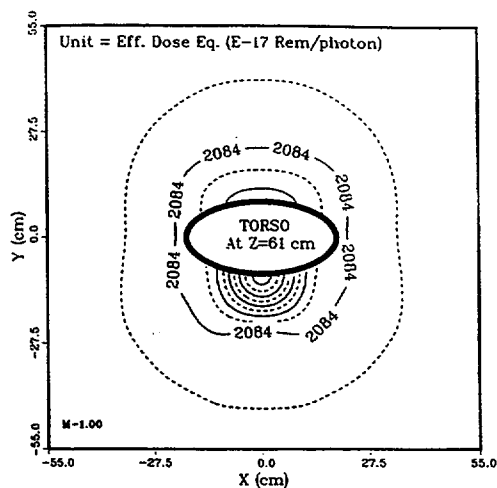
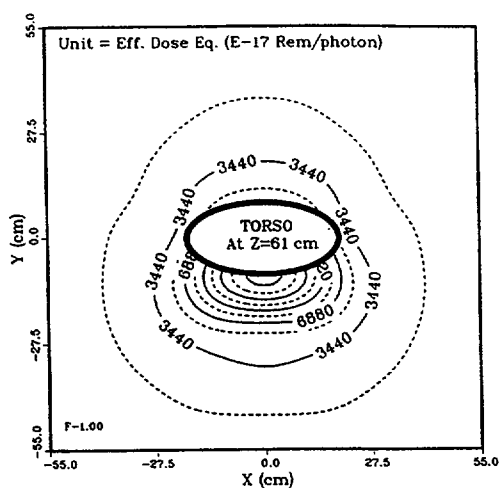


Figure 16. Contour plots of H_E for a female vs. source location for a 1.0 MeV point source

Figure 17. Contour plots of H_E for a male vs. source location for a 1.0 MeV point source

4

CONCLUSIONS AND FUTURE WORK

4.1 Conclusions of Phase I

This report documents an approach that can be used to formulate a rational methodology for assessing effective dose equivalent (H_E) from external photon exposures. It presents organ doses and effective dose equivalent (calculated from organ doses) for both beam sources and point sources radiating from any direction or position in three-dimensional space. Although the data presented here are only a part of the EPRI effective dose equivalent study, several conclusions are already evident.

For beam or point source geometry, H_E decreases with decreasing photon energy, principally because of shielding by the intervening tissues. This continuous decrease is in contrast to the increase in dose (1 cm deep) at low photon energies predicted by the ANSI Standard used by the industry. For equal beam intensities, radiation striking the body from the front (the anterior-posterior or AP direction) produces the greatest effective dose equivalent. Beams striking the rear of the torso (the PA direction) produce the next highest effective dose equivalent, with effective dose equivalent falling significantly as one departs from these two orientations.

Point sources are shown to be relatively innocuous compared to the uniform exposure from beams. Flux from a point source falls as the reciprocal of the distance from the source squared. Point sources close to the torso generate small doses for organs and tissues proximal to the source because of this rapid decrease in the flux. This is true even if shielding by intervening tissues is ignored. The effective dose equivalent drops orders of magnitude for sources a foot or more away from contact with the torso. For point sources the highest effective dose equivalent for females occurs when the source is in contact

with the body on the sternum, for males when the source is on the gonads. For all photon energies, effective dose equivalent is always higher for a point source on the male gonads than it is for the same source on the sternum of the female.

Questions have been raised as to the adequacy of radiation workers' dosimetry, in particular whether or not their dosimetry is at or near the point of highest exposure on the torso. Indeed, the NRC has cited some utilities for not having dosimeters at the point of highest dose. This concern has led to the widespread practice of multi-badging radiation workers and assigning the highest dose among the multiple dosimeters as the dose of record. This study shows that practice to be overly conservative. As the angle of beam incidence is changed from AP, effective dose equivalent drops dramatically. The drop-off is often more than the under-response of a dosimeter, thus dosimeters will not under predict H_E regardless of the incident photon angle. Moreover, dosimeters worn at the points of highest dose on the surface over-respond, since they are calibrated for AP exposures that produce the highest dose per unit fluence.

A recent report by the NCRP¹³ recommends a limit of 75 microcurie-hours for small beta-emitting sources ("hot particles"). There has also been concern expressed over the potential for photon dose from these hot particles. This study shows that for point sources emitting 1.0 MeV photons in contact with the torso at the worst locations (on the sternum for the female and on the gonads for the male), effective dose equivalent is approximately 5 millirem for a 75 microcurie-hour exposure. Because ⁶⁰Co emits two photons per disintegration, cobalt point sources at these worst locations would produce a dose of

about 10 millirem. Other locations on the body will have an effective dose equivalent one to two orders of magnitude lower.

We have demonstrated that using industry standard codes and realistic phantoms it is possible to accurately assess effective dose equivalent from external photon exposures. Using this approach will eliminate the overly conservative exposure estimates resulting from current dosimetry practices, and will provide radiation exposures that realistically estimate the risk of radiation injury. The data summarized in this report and contained in the appendices can be used by advisory groups to establish recommendations for protecting radiation workers from external radiation fields.

4.2 Future Work

MCNP calculations of surface energy and surface photon fluxes for point and beam geometries as a function of gender and photon energy are nearly complete. Work

is underway to develop algorithms for converting surface energy fluxes to effective dose equivalent. These algorithms will allow dosimeter measurements of external radiation to be directly converted to estimates of effective dose equivalent using the data presented in this report. Dose and surface flux measurements have also been made on a male physical phantom (RANDO™). The measurements were done at a commercial pressurized water reactor in order to use typical radiation fields. These measurements of H_E are being analyzed and will be compared to H_E values calculated using the algorithms. When this additional work is published in 1993, we expect that the methodology will exist to allow a worker's effective dose equivalent to be accurately estimated from one (or at most a few) dosimeter measurements. This will still yield a conservative estimate of the risk of radiation exposure, but will eliminate many of the often large differences between the dose equivalent as conveniently determined at one cm depth, and the dose equivalents actually received by internal organs.

5

REFERENCES

-
1. Title 10 Part 20 of the Code of Federal Regulations, "Standards for Protection Against Radiation," as revised August 21, 1991.
 2. International Commission on Radiological Protection, "Recommendations of the International Commission on Radiological Protection," ICRP Publication 26, Annals of the ICRP, Vol. 1 No. 3, Pergamon Press, 1977.
 3. International Commission on Radiological Protection, "Problems Involved in Developing an Index of Harm," ICRP Publication 27, Annals of the ICRP, Vol. 1 No. 4, Pergamon Press, 1977.
 4. Title 10 Part 20 of the Code of Federal Regulations, § 20.1003.
 5. Nuclear Regulatory Commission, Regulatory Guide 8.34, "Monitoring Criteria and Methods to Calculate Occupational Radiation Doses," June 1992.
 6. M. Cristy and K.F. Eckerman, "Specific Absorbed Fractions of Energy at Various Ages from Internal Photon Sources," ORNL/TM-8381/V1, April, 1987.
 7. J.J. Kelly, "Experiences in Limiting Radiation Exposure to the Embryo/Fetus in Nuclear Power Plants," Proceedings of the Twenty-Fourth Mid-Year Topical Meeting of the Health Physics Society, Raleigh, NC, January 21-24, 1991.
 8. International Commission on Radiological Protection, "Data for Use in Protection Against External Radiation," ICRP Publication 51, Annals of the ICRP, Vol. 17 No. 2/3, Pergamon Press, 1987.
 9. R. Kramer and G. Drexler, "On the Calculation of the Effective Dose Equivalent," Radiation Protection Dosimetry, Vol. 3 No. 1/2, 1982.
 10. Radiation Shielding Information Center, "MCNP 4: Monte Carlo Neutron and Photon Transport Code System," Oak Ridge National Laboratory Report No. CCC-200A, 1991.
 11. K.L. Jones, et al, "Performance Criteria for Dosimeter Angular Response," PNL-6452, Battelle Pacific Northwest Laboratory, June 1988.
 12. American Nuclear Society, "American National Standard Neutron and Gamma-Ray Flux-to-Dose-Rate Factors," ANSI/ANS-6.1.1-1977, 1977
 13. National Council on Radiation Protection and Measurements, "Limit for Exposure to 'Hot Particles' on the Skin," NCRP Report No. 106, 1989.



ATTACHMENT 1

SUPPORTING GRAPHICS AND TABLES

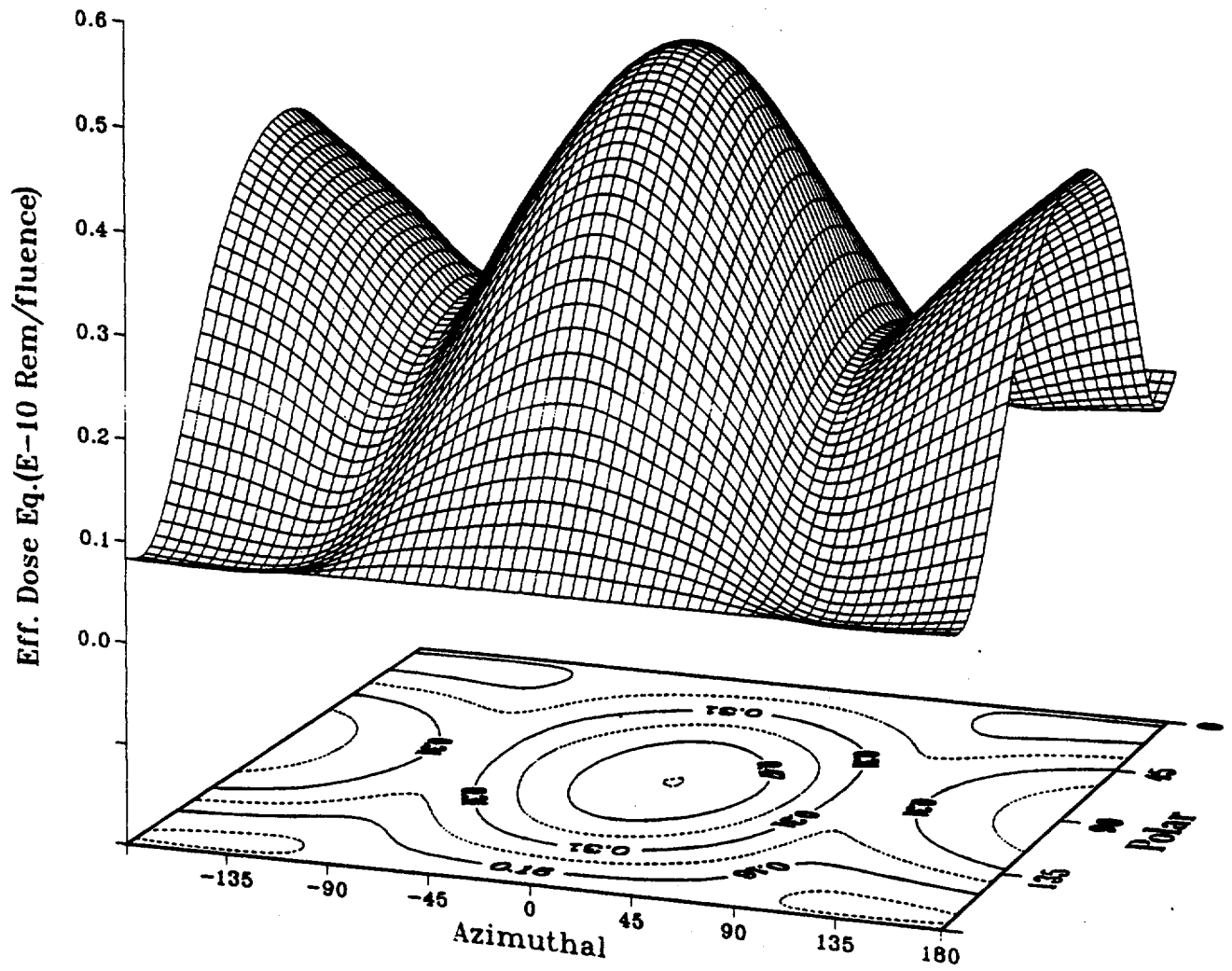


Figure A1-1. Surface and contour plots of effective dose equivalent for a female for 0.08 MeV photon beams

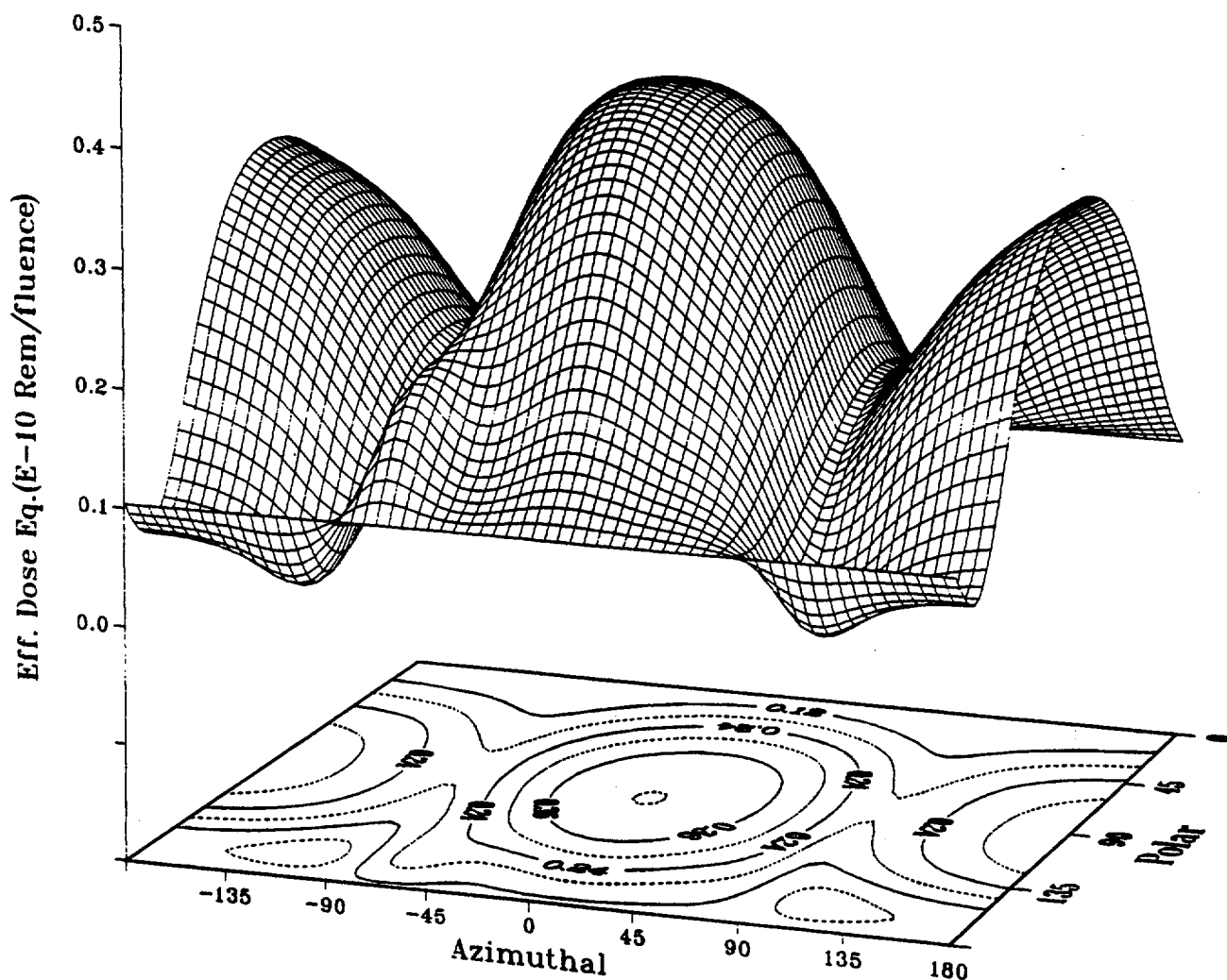


Figure A1-2. Surface and contour plots of effective dose equivalent for a male for 0.08 MeV photon beams

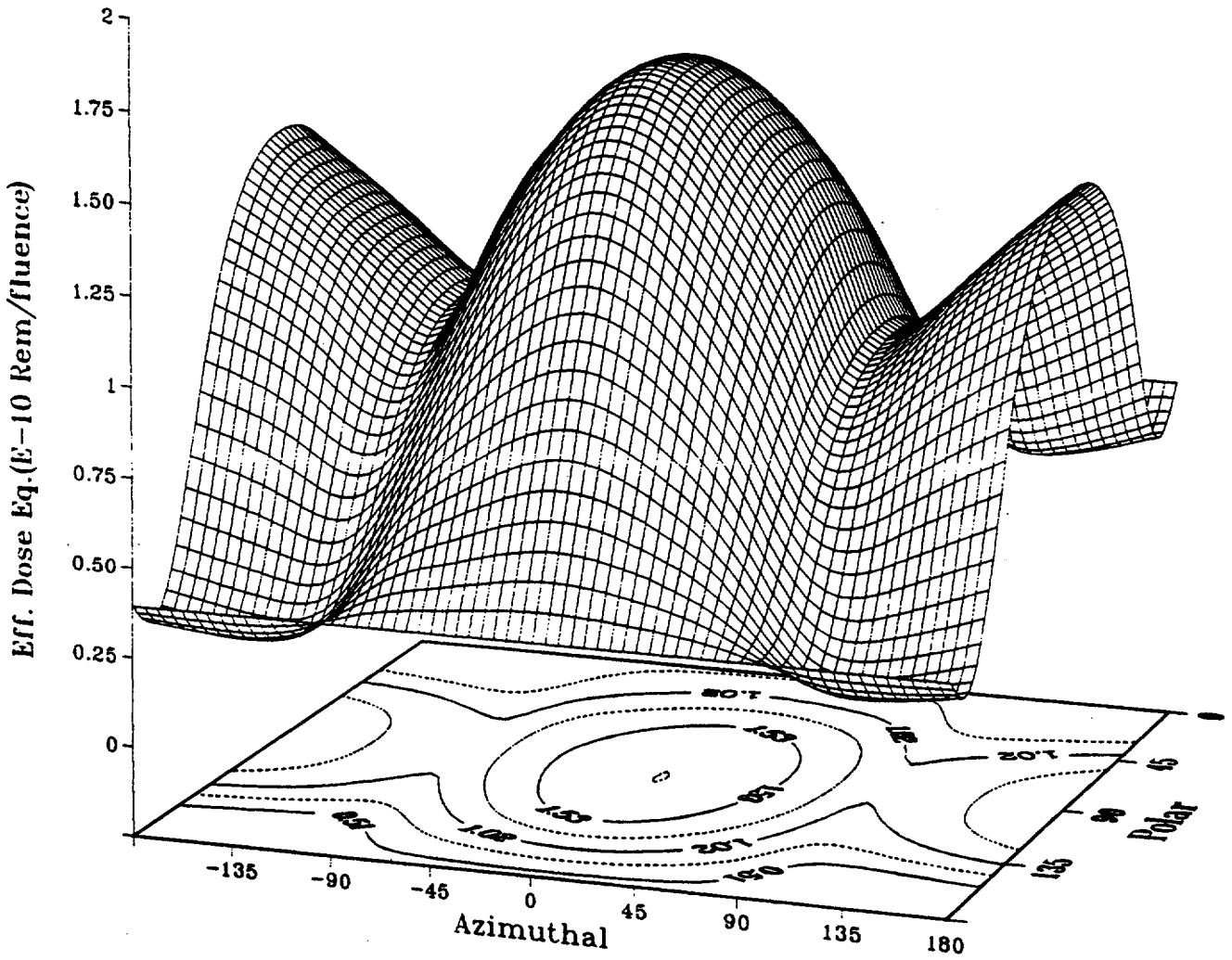


Figure A1-3. Surface and contour plots of effective dose equivalent for a female for 0.3 MeV photon beams

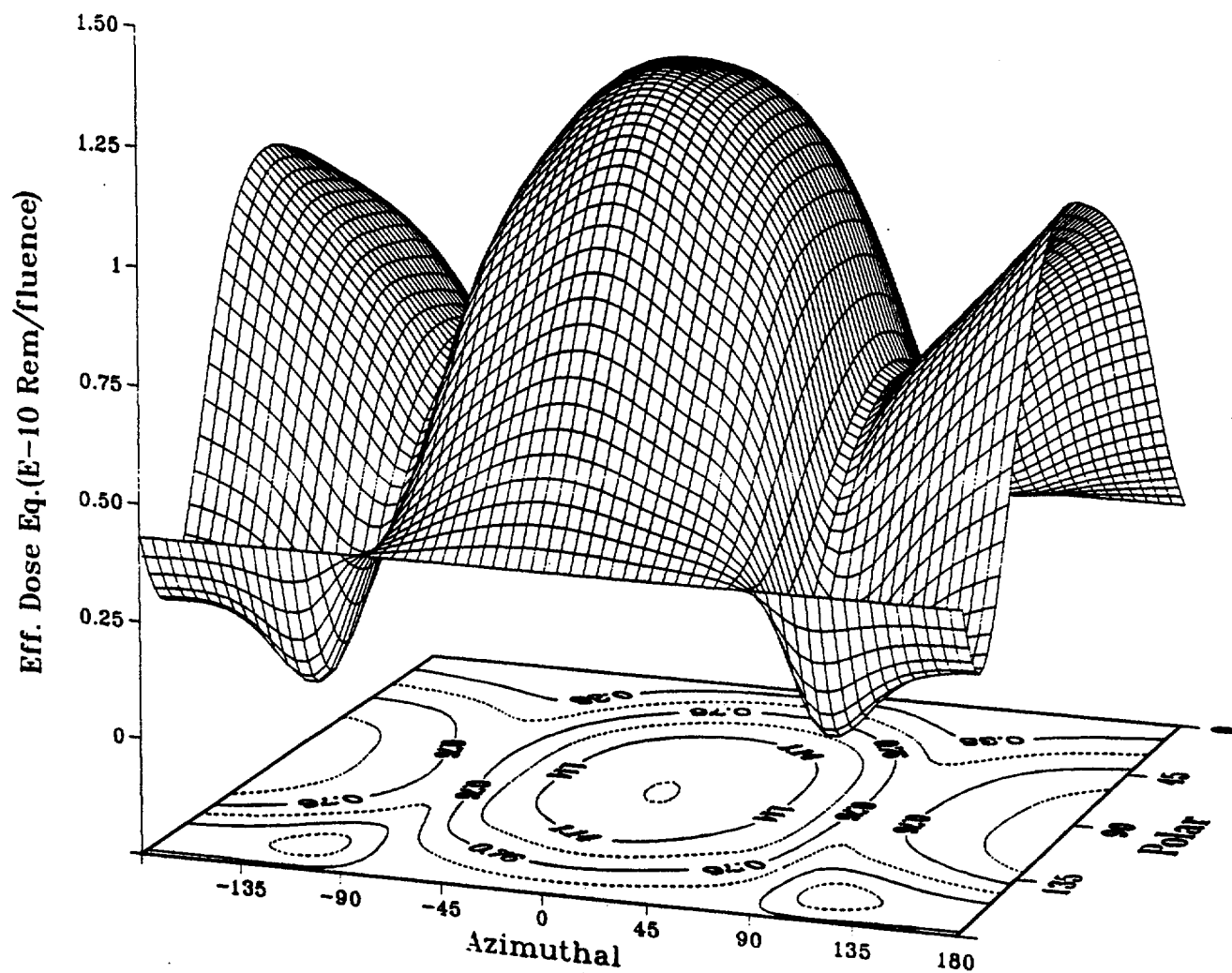
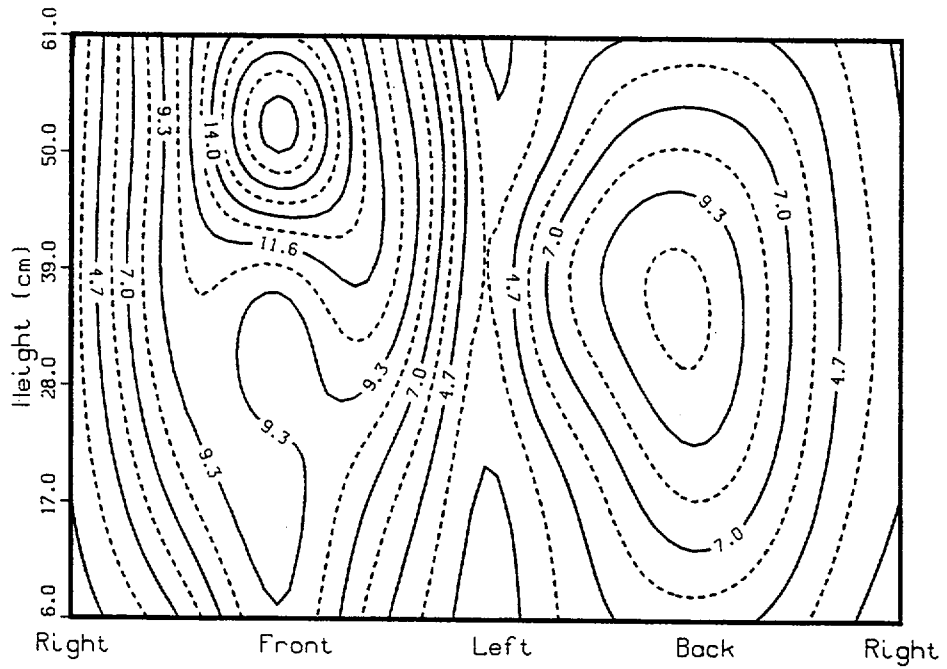
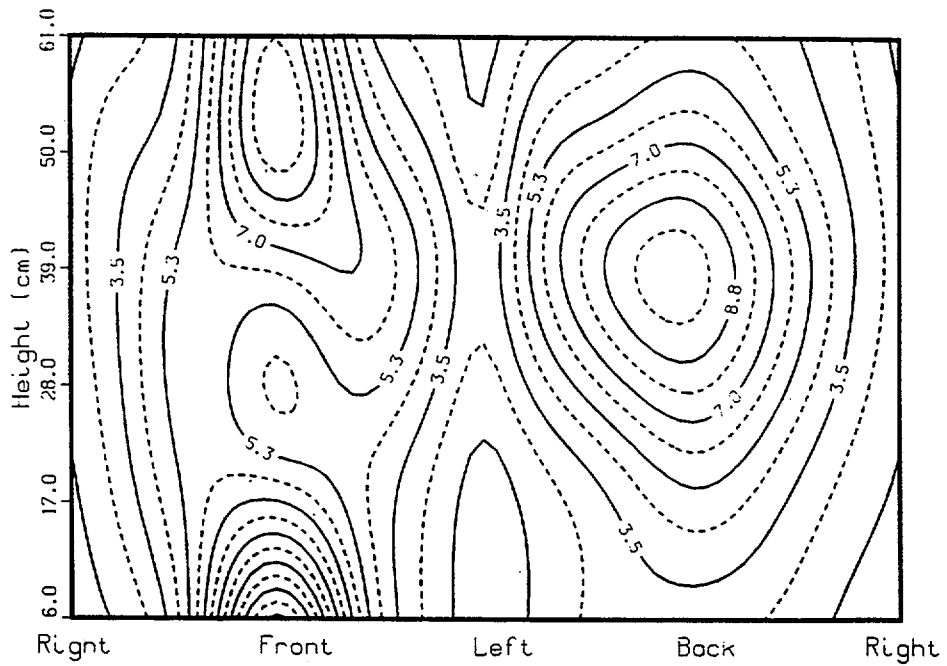


Figure A1-4. Surface and contour plots of effective dose equivalent for a male for 0.3 MeV photon beams



Female



Male

Figure A1-5. Contour plots of H_E for 0.08 MeV point sources in contact with the body (units = 10^{-15} rem/photon emitted)

Table A1-1

Effective Dose Equivalent for Point Sources Located 6 cm Above the Data Plane* that are Emitting 0.08 MeV Photons (units = E-17 rad per photon emitted)

Adult Female

X (cm)*	-55	-44	-33	-22	-11	0	11	22	33	44	55
Y (cm)*											
55	37.9	47.9	58.7	70.4	77.7	79.9	77.7	70.4	58.7	47.9	37.9
44	41.7	55.0	71.4	90.0	107.2	108.8	107.2	90.0	71.4	55.0	41.7
33	43.0	60.1	85.0	117.4	150.8	162.5	150.8	117.4	85.0	60.1	43.0
22	46.1	64.2	93.5	152.8	232.4	276.7	232.4	152.8	93.5	64.2	46.1
11	47.2	63.4	91.9	180.4	409.9	520.0	409.9	180.4	91.9	63.4	47.2
0	46.1	60.8	89.0	156.2				156.2	89.0	60.8	46.1
-11	51.8	72.9	113.9	217.0	524.4	919.0	524.0	217.0	113.9	72.9	51.8
-22	58.1	81.0	121.8	197.5	305.1	370.7	305.0	197.5	121.8	81.0	58.1
-33	58.9	78.3	111.0	153.3	192.1	212.2	192.1	153.3	111.0	78.3	58.9
-44	54.9	71.7	91.4	115.8	136.3	141.5	136.3	115.8	91.4	71.7	54.9
-55	49.6	60.9	74.7	86.9	99.1	102.3	99.1	86.9	74.7	60.9	49.6

Adult Male

X (cm)*	-55	-44	-33	-22	-11	0	11	22	33	44	55
Y (cm)*											
55	30.6	37.3	46.0	54.7	60.9	62.6	60.9	54.7	46.0	37.3	30.6
44	33.0	42.7	55.2	69.7	81.0	84.5	81.0	69.7	55.2	42.7	33.0
33	33.2	46.5	65.0	88.7	110.0	117.1	110.0	88.7	65.0	46.5	33.2
22	33.5	47.3	70.0	110.5	160.2	183.8	160.2	110.5	70.0	47.3	33.5
11	30.8	42.8	65.1	122.1	261.2	301.4	261.2	122.1	65.1	42.8	30.8
0	30.3	41.5	60.2	115.7				115.7	60.2	41.5	30.3
-11	35.2	51.6	87.2	189.6	573.0	1429.0	573.0	189.6	87.2	51.6	35.2
-22	44.9	68.6	115.6	212.1	407.2	553.2	407.2	212.1	115.6	68.6	44.9
-33	49.9	71.4	106.3	162.3	226.9	263.0	226.9	162.3	106.3	71.4	49.9
-44	47.2	64.3	88.5	115.0	142.8	150.3	142.8	115.0	88.5	64.3	47.2
-55	43.0	55.1	67.4	83.8	94.7	97.7	94.7	83.8	67.4	55.1	43.0

* See Figure 12 in the main text for the explanation of the coordinate system.

Table A1-2

Effective Dose Equivalent for Point Sources Located 6 cm Above the Data Plane* that are Emitting 0.3 MeV Photons (units = E-17 rad per photon emitted)

Adult Female

X (cm)*	-44	-33	-22	-11	0	11	22	33	44
Y (cm)*									
44	193.2	245.7	305.9	355.4	373.3	355.4	305.9	245.7	193.2
33	216.1	301.6	411.9	514.4	550.7	514.4	411.9	301.6	216.1
22	240.9	347.5	551.5	801.7	934.9	801.7	551.5	347.5	240.9
11	258.2	366.3	675.0	1440.0	1819.0	1440.0	675.0	366.3	258.2
0	266.3	381.7	695.6				695.6	381.7	266.3
-11	302.6	476.1	841.5	1856.0	3221.0	1856.0	841.5	476.1	302.6
-22	311.7	462.3	722.2	1078.0	1262.0	1078.0	722.2	462.3	311.7
-33	302.1	399.5	543.7	666.7	740.6	666.7	543.7	399.5	302.1
-44	257.3	326.8	406.8	469.1	493.9	469.1	406.8	326.8	257.3

Adult Male

X (cm)*	-44	-33	-22	-11	0	11	22	33	44
Y (cm)*									
44	145.70	184.20	229.90	266.40	275.70	266.40	229.90	184.20	145.70
33	167.70	225.00	297.80	366.10	390.30	366.10	297.80	225.00	167.70
22	173.40	257.30	392.70	546.50	615.40	546.60	392.70	257.30	173.40
11	174.80	269.40	476.40	929.90	1081.00	929.90	476.40	269.40	174.80
0	184.10	269.90	503.80				503.80	269.90	184.10
-11	214.90	374.40	773.20	2130.00	5204.00	2130.00	773.20	374.40	214.90
-22	261.00	438.50	776.60	1398.00	1870.00	1398.00	776.60	438.50	261.00
-33	260.00	380.20	548.20	760.30	868.10	760.30	548.20	380.20	260.00
-44	224.40	300.10	381.50	464.20	488.60	464.20	381.50	300.10	224.40

* See Figure 12 in the main text for the explanation of the coordinate system.

Table A1-3

Effective Dose Equivalent for Point Sources Located 6 cm Above the Data Plane* that are Emitting 1.0 MeV Photons (units = E-17 rad per photon emitted)

Adult Female

X (cm)*	-44	-33	-22	-11	0	11	22	33	44
Y (cm)*									
44	643.8	821.4	975.7	1116.0	1169.0	1116.0	975.7	821.4	643.8
33	742.2	1020.0	1352.0	1657.0	1773.0	1657.0	1352.0	1020.0	742.2
22	879.5	1247.0	1850.0	2624.0	3028.0	2624.0	1850.0	1247.0	879.5
11	948.6	1390.0	2471.0	4874.0	6071.0	4874.0	2471.0	1390.0	948.6
0	979.3	1501.0	2643.0				2643.0	1501.0	979.3
-11	1086.0	1697.0	2966.0	6110.0	10390.0	6110.0	2966.0	1697.0	1086.0
-22	1061.0	1513.0	2349.0	3384.0	3976.0	3384.0	2349.0	1513.0	1061.0
-33	955.2	1268.0	1704.0	2073.0	2269.0	2073.0	1704.0	1268.0	955.2
-44	827.5	1012.0	1280.0	1419.0	1500.0	1419.0	1280.0	1012.0	827.5

Adult Male

X (cm)*	-44	-33	-22	-11	0	11	22	33	44
Y (cm)*									
44	492.9	613.9	746.9	841.7	884.8	841.7	746.9	613.9	492.9
33	579.5	770.3	994.2	1209.0	1285.0	1209.0	994.2	770.3	579.5
22	639.0	928.5	1382.0	1897.0	2079.0	1897.0	1382.0	928.5	639.0
11	684.8	1046.0	1787.0	3293.0	3840.0	3293.0	1787.0	1046.0	684.8
0	749.6	1131.0	2083.0				2083.0	1131.0	749.6
-11	822.9	1407.0	2735.0	7141.0	16850.0	7141.0	2735.0	1407.0	822.9
-22	888.4	1433.0	2429.0	4235.0	5589.0	4235.0	2429.0	1433.0	888.4
-33	825.5	1171.0	1665.0	2264.0	2563.0	2264.0	1665.0	1171.0	825.5
-44	690.7	908.7	1139.0	1368.0	1443.0	1368.0	1139.0	908.7	690.7

* See Figure 12 in the main text for the explanation of the coordinate system.

Table A1-4

Effective Dose Equivalent for Point Sources Located 41 cm Above the Data Plane* that are Emitting 0.08 MeV Photons (units = E-17 rad per photon emitted)

Adult Female

X (cm)*	-44	-33	-22	-11	0	11	22	33	44
Y (cm)*									
44	69.1	91.3	118.8	141.5	148.5	141.5	118.8	91.3	69.1
33	79.9	117.9	170.2	219.1	238.7	219.1	170.2	117.9	79.9
22	92.6	142.5	247.3	382.9	435.0	382.9	247.3	142.5	92.6
11	99.8	158.3	338.8	836.5	1036.0	836.5	338.8	158.3	99.8
0	103.4	177.5	329.0				329.0	177.5	103.4
-11	119.8	216.9	497.4	1128.0	1150.0	1128.0	497.4	216.9	119.8
-22	123.9	204.6	368.5	572.5	639.3	572.5	368.5	204.6	123.9
-33	111.4	164.9	240.7	315.8	349.4	315.8	240.7	164.9	111.4
-44	94.8	128.3	163.5	198.1	209.5	198.1	163.5	128.3	94.8

Adult Male

X (cm)*	-44	-33	-22	-11	0	11	22	33	44
Y (cm)*									
44	55.6	74.7	96.0	113.7	119.2	113.7	96.0	74.7	55.6
33	65.2	96.5	140.6	180.8	195.9	180.8	140.6	96.5	65.2
22	70.8	118.9	211.0	331.3	374.8	331.3	211.0	118.9	70.8
11	67.6	124.6	300.8	770.6	984.0	770.6	300.8	124.6	67.6
0	61.2	106.3	261.6				261.6	106.3	61.2
-11	66.1	113.6	251.0	611.4	700.1	611.4	251.3	113.6	66.1
-22	71.7	112.9	189.0	287.3	338.3	287.3	189.0	112.9	71.7
-33	68.5	99.6	137.8	179.1	198.5	179.1	137.8	99.6	68.5
-44	61.4	81.2	102.7	122.7	131.1	122.7	102.7	81.2	61.4

* See Figure 12 in the main text for the explanation of the coordinate system.

Table A1-5

Effective Dose Equivalent for Point Sources Located 41 cm Above the Data Plane* that are Emitting 0.3 MeV Photons (units = E-17 rad per photon emitted)

Adult Female

X (cm)*	-44	-33	-22	-11	0	11	22	33	44
Y (cm)*									
44	233.7	312.4	402.4	475.8	501.7	475.8	402.4	312.4	233.7
33	287.3	412.2	578.0	739.8	793.5	739.8	578.2	412.2	287.3
22	345.3	519.4	866.0	1300.0	1462.0	1300.0	866.0	519.4	345.3
11	385.9	619.6	1258.0	3006.0	3622.0	3006.0	1258.0	619.6	385.9
0	418.4	733.7	1448.0				1448.0	733.7	418.4
-11	473.9	848.0	1900.0	4158.0	4286.0	4158.0	1900.0	848.0	473.9
-22	473.3	762.5	1343.0	2062.0	2278.0	2062.0	1343.0	762.5	473.3
-33	407.1	599.0	865.1	1110.0	1210.0	1110.0	865.1	599.0	407.1
-44	335.8	449.2	565.6	674.8	721.7	674.8	565.6	449.2	335.8

Adult Male

X (cm)*	-44	-33	-22	-11	0	11	22	33	44
Y (cm)*									
44	177.0	235.0	292.6	349.0	364.8	349.0	292.6	235.0	177.0
33	214.5	310.9	440.7	559.0	600.8	559.0	440.7	310.9	214.5
22	241.3	396.1	679.0	1052.0	1183.0	1052.0	679.0	396.1	241.3
11	245.2	448.3	1053.0	2642.0	3297.0	2642.0	1053.0	448.3	245.2
0	238.5	419.5	1066.0				1066.0	419.5	238.5
-11	256.6	434.8	915.9	2106.0	2404.0	2106.0	915.9	434.8	256.6
-22	267.2	409.5	658.5	992.5	1144.0	992.5	658.5	409.5	267.2
-33	244.4	351.8	467.8	616.3	661.1	616.3	467.8	351.8	244.4
-44	207.2	275.6	346.1	397.6	430.8	397.6	346.1	275.6	207.2

* See Figure 12 in the main text for the explanation of the coordinate system.

Table A1-6

Effective Dose Equivalent for Point Sources Located 41 cm Above the Data Plane* that are Emitting 1.0 MeV Photons (units = E-17 rad per photon emitted)

Adult Female

X (cm)*	-44	-33	-22	-11	0	11	22	33	44
Y (cm)*									
44	787.5	1019.0	1278.0	1488.0	1586.0	1488.0	1278.0	1019.0	787.5
33	974.5	1362.0	1865.0	2347.0	2542.0	2347.0	1865.0	1362.0	974.5
22	1182.0	1775.0	2844.0	4178.0	4690.0	4178.0	2844.0	1775.0	1182.0
11	1386.0	2220.0	4388.0	9894.0	12020.0	9894.0	4388.0	2220.0	1386.0
0	1486.0	2626.0	5469.0				5469.0	2626.0	1486.0
-11	1628.0	2882.0	6247.0	13290.0	13800.0	13290.0	6247.0	2882.0	1628.0
-22	1552.0	2470.0	4247.0	6469.0	7094.0	6469.0	4247.0	2470.0	1552.0
-33	1302.0	1905.0	2639.0	3393.0	3722.0	3393.0	2639.0	1905.0	1302.0
-44	1054.0	1400.0	1751.0	2051.0	2100.0	2051.0	1751.0	1400.0	1054.0

Adult Male

X (cm)*	-44	-33	-22	-11	0	11	22	33	44
Y (cm)*									
44	569.7	725.1	909.6	1052.0	1106.0	1052.0	909.6	725.1	569.7
33	709.5	985.5	1367.0	1715.0	1841.0	1715.0	1367.0	985.5	709.5
22	822.2	1309.0	2167.0	3232.0	3646.0	3232.0	2167.0	1309.0	822.2
11	882.3	1570.0	3471.0	8467.0	10670.0	8467.0	3471.0	1570.0	882.3
0	880.1	1547.0	3895.0				3895.0	1547.0	880.1
-11	928.4	1549.0	3125.0	6907.0	7925.0	6907.0	3125.0	1549.0	928.4
-22	902.4	1346.0	2137.0	3110.0	3579.0	3110.0	2137.0	1346.0	902.4
-33	783.1	1099.0	1457.0	1853.0	1997.0	1853.0	1457.0	1099.0	783.1
-44	649.7	846.9	1039.0	1209.0	1220.0	1209.0	1039.0	846.9	649.7

* See Figure 12 in the main text for the explanation of the coordinate system.

Table A1-7

Effective Dose Equivalent for Point Sources Located 61 cm Above the Data Plane* that are Emitting 0.08 MeV Photons (units = E-17 rad per photon emitted)

Adult Female

X (cm)*	-55	-44	-33	-22	-11	0	11	22	33	44	55
Y (cm)*											
55	40.3	50.7	62.7	73.4	82.8	86.5	82.8	73.4	62.7	50.7	40.3
44	45.9	59.5	77.2	96.4	112.8	119.1	112.8	96.4	77.2	59.5	45.9
33	51.1	67.0	94.1	129.3	161.3	175.2	161.3	129.3	94.1	67.0	51.1
22	55.0	74.9	107.5	166.7	240.4	271.5	240.4	166.7	107.5	74.9	55.0
11	59.8	82.4	115.6	200.5	414.2	511.0	414.2	200.5	115.6	82.4	59.8
0	63.2	91.5	145.9	209.0				209.0	145.9	91.5	63.2
-11	69.2	107.1	191.0	440.0	1114.0	1521.0	1114.0	440.0	191.0	107.1	69.2
-22	75.6	116.4	190.2	340.6	552.2	634.0	552.0	340.0	190.0	116.4	75.6
-33	74.0	104.9	153.6	224.8	296.1	323.3	296.1	224.8	153.6	104.9	74.0
-44	66.0	89.2	116.9	152.9	181.2	195.4	181.2	152.9	116.9	89.2	66.0
-55	57.2	71.8	90.7	107.7	122.8	129.8	122.8	107.7	90.7	71.8	57.2

Adult Male

X (cm)*	-55	-44	-33	-22	-11	0	11	22	33	44	55
Y (cm)*											
55	33.3	41.4	51.0	60.1	66.9	68.9	66.9	60.1	51.0	41.4	33.3
44	37.1	49.0	64.1	80.2	93.0	97.0	93.0	80.2	64.1	49.0	37.1
33	39.5	55.3	79.7	109.7	136.1	145.5	136.1	109.7	79.7	55.3	39.5
22	40.0	58.5	90.3	144.3	208.1	234.8	208.1	144.3	90.3	58.5	40.0
11	38.4	55.3	88.0	171.4	357.2	462.0	357.2	171.4	88.0	55.3	38.4
0	37.2	51.5	75.1	149.5				149.5	75.1	51.5	37.2
-11	38.5	55.1	87.1	165.0	380.0	961.0	380.0	165.0	87.1	55.1	38.5
-22	41.3	60.2	91.7	145.5	231.7	299.8	231.7	145.5	91.7	60.2	41.3
-33	42.6	58.2	82.0	113.7	148.1	164.0	148.1	113.7	82.0	58.2	42.6
-44	40.9	52.7	68.2	85.9	101.6	109.2	101.6	85.9	68.2	52.7	40.9
-55	36.9	45.8	56.4	66.4	74.4	77.6	74.4	66.4	56.4	45.8	36.9

* See Figure 12 in the main text for the explanation of the coordinate system.

Table A1-8

Effective Dose Equivalent for Point Sources Located 61 cm Above the Data Plane* that are Emitting 0.3 MeV Photons (units = E-17 rad per photon emitted)

Adult Female

X (cm)*	-44	-33	-22	-11	0	11	22	33	44
Y (cm)*									
44	207.6	262.6	327.1	383.2	405.6	383.2	327.1	262.6	207.6
33	240.3	329.6	438.6	545.9	582.4	545.9	438.6	329.6	240.3
22	278.7	390.3	590.2	821.5	915.6	821.5	590.2	390.3	278.7
11	329.3	458.3	752.9	1419.0	1628.0	1419.0	752.9	458.3	329.3
0	368.2	599.3	937.3				937.3	599.3	368.2
-11	423.9	749.3	1700.0	4212.0	5633.0	4212.0	1700.0	749.3	423.9
-22	435.2	712.3	1261.0	2020.0	2275.0	2020.0	1261.0	712.3	435.2
-33	384.4	558.9	796.1	1040.0	1139.0	1040.0	796.1	558.9	384.4
-44	317.7	414.6	538.5	630.7	673.5	630.7	538.5	414.6	317.7

Adult Male

X (cm)*	-44	-33	-22	-11	0	11	22	33	44
Y (cm)*									
44	155.4	200.3	246.5	282.3	295.8	282.3	246.5	200.3	155.4
33	180.0	253.8	337.7	416.9	442.4	416.9	337.7	253.8	180.0
22	197.3	299.1	462.4	644.7	715.5	644.7	462.4	299.1	197.3
11	198.7	312.9	587.9	1124.0	1344.0	1124.0	587.9	312.9	198.7
0	193.6	292.0	539.0				539.0	292.0	193.6
-11	210.7	328.8	601.4	1320.0	3393.0	1320.0	601.4	328.8	210.7
-22	220.4	327.8	511.6	790.1	1002.0	790.1	511.6	327.8	220.4
-33	207.3	285.8	381.5	488.9	542.3	488.9	381.5	285.8	207.3
-44	181.7	230.2	288.5	333.5	354.3	333.5	288.5	230.2	181.7

* See Figure 12 in the main text for the explanation of the coordinate system.

Table A1-9

Effective Dose Equivalent for Point Sources Located 61 cm Above the Data Plane* that are Emitting 1.0 MeV Photons (units = E-17 rad per photon emitted)

Adult Female

X (cm)*	-44	-33	-22	-11	0	11	22	33	44
Y (cm)*									
44	699.5	879.4	1081.0	1249.0	1319.0	1249.0	1081.0	879.4	699.5
33	836.6	1110.0	1464.0	1805.0	1932.0	1805.0	1464.0	1110.0	836.6
22	997.9	1392.0	2041.0	2773.0	3097.0	2773.0	2041.0	1392.0	997.9
11	1181.0	1711.0	2812.0	4933.0	5761.0	4933.0	2812.0	1711.0	1181.0
0	1314.0	2172.0	3693.0				3693.0	2172.0	1314.0
-11	1459.0	2559.0	5591.0	13510.0	17900.0	13510.0	5591.0	2559.0	1459.0
-22	1431.0	2301.0	4008.0	6318.0	7072.0	6318.0	4008.0	2301.0	1431.0
-33	1225.0	1770.0	2464.0	3201.0	3489.0	3201.0	2464.0	1770.0	1225.0
-44	997.6	1288.0	1638.0	1929.0	2044.0	1929.0	1638.0	1288.0	997.6

Adult Male

X (cm)*	-44	-33	-22	-11	0	11	22	33	44
Y (cm)*									
44	500.9	630.2	768.7	875.6	910.6	875.6	768.7	630.2	500.9
33	594.9	812.0	1072.0	1300.0	1379.0	1300.0	1072.0	812.0	594.9
22	671.7	992.3	1509.0	2062.0	2279.0	2062.0	1509.0	992.3	671.7
11	712.7	1110.0	2038.0	3767.0	4544.0	3767.0	2038.0	1110.0	712.7
0	721.6	1128.0	2082.0				2082.0	1128.0	721.6
-11	768.8	1202.0	2110.0	4429.0	10920.0	4429.0	2110.0	1202.0	768.8
-22	758.4	1113.0	1687.0	2510.0	3132.0	2510.0	1687.0	1113.0	758.4
-33	680.5	919.2	1209.0	1524.0	1670.0	1524.0	1209.0	919.2	680.5
-44	575.5	722.0	878.2	1022.0	1082.0	1022.0	878.2	722.0	575.5

* See Figure 12 in the main text for the explanation of the coordinate system.

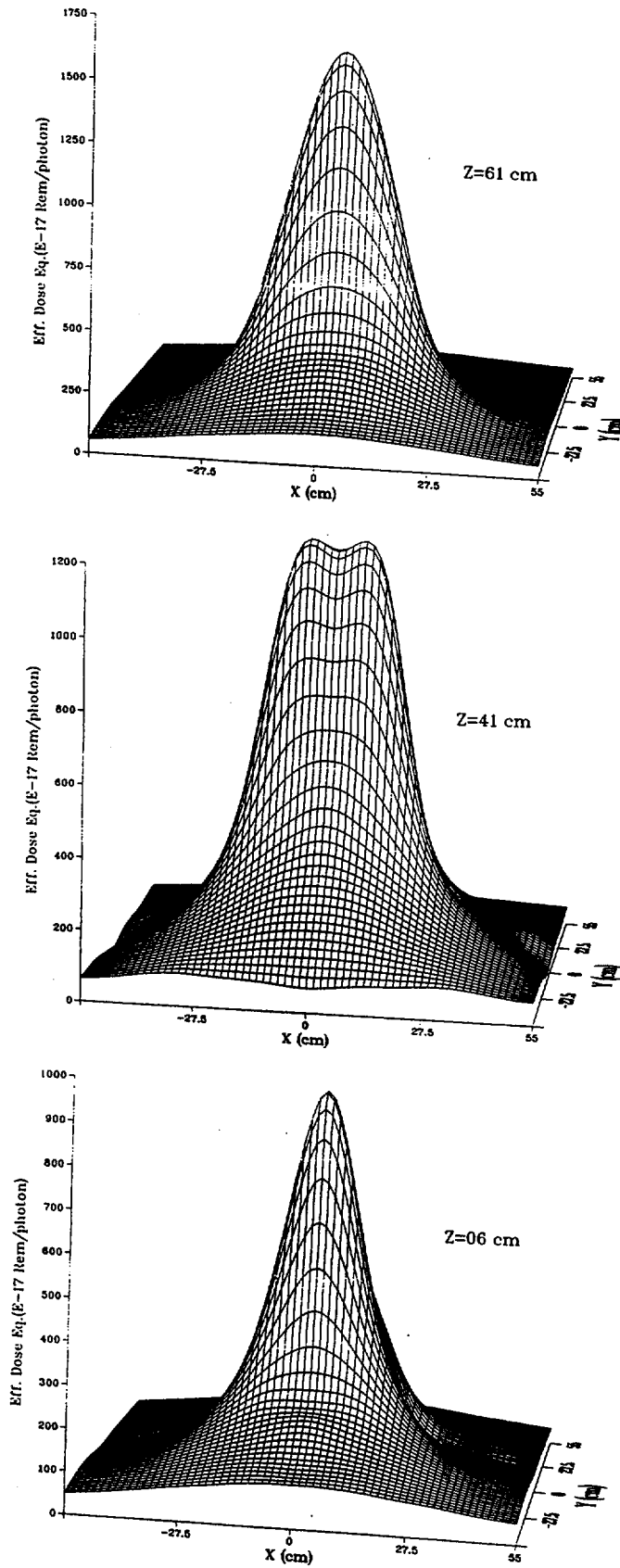
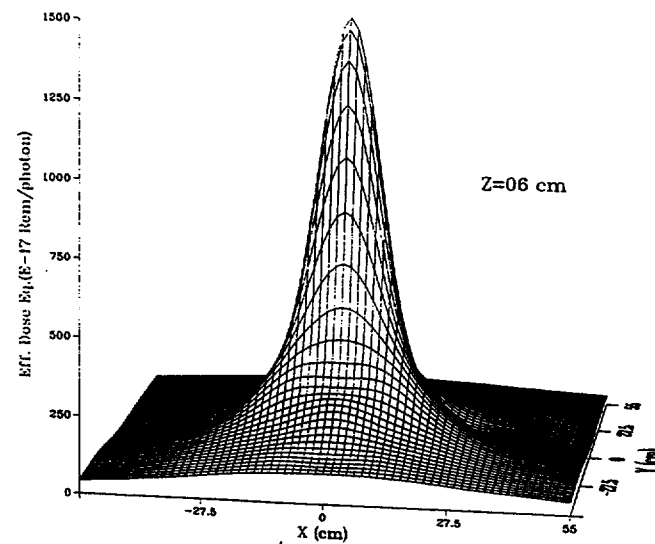
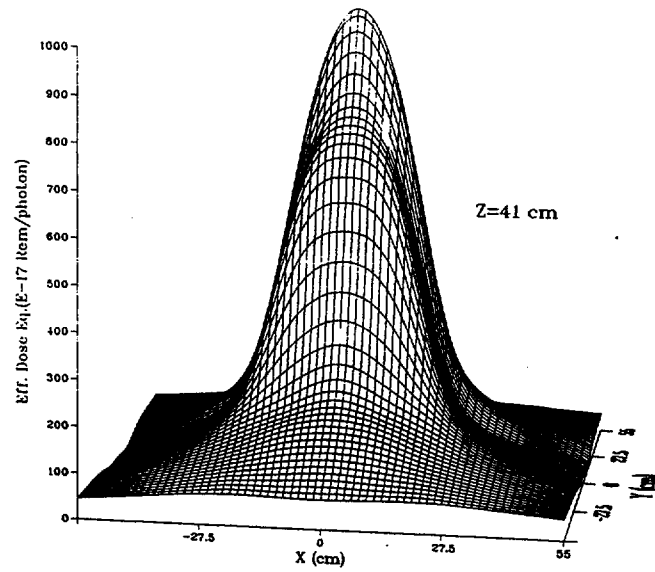
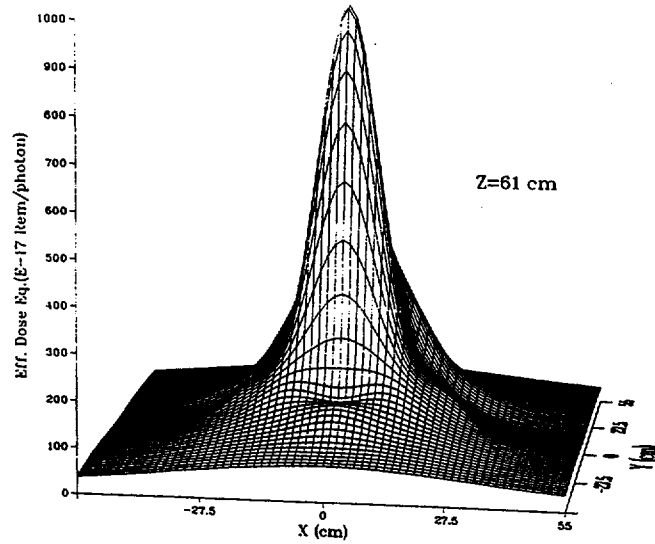


Figure A1-7. Surface plots of H_E for a female vs. source location for a 0.08 MeV point source



A1-18

Figure A1-8. Surface plots of H_E for a male vs. source location for a 0.08 MeV point source

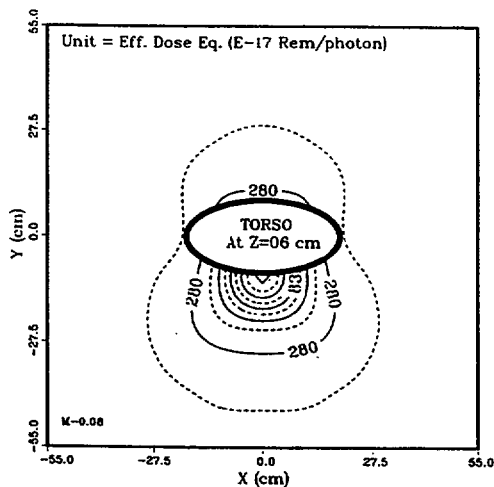
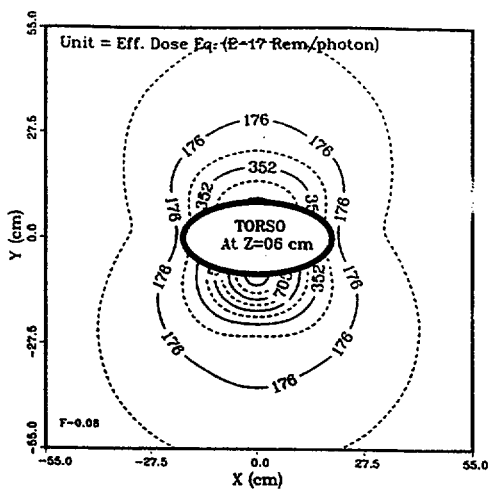
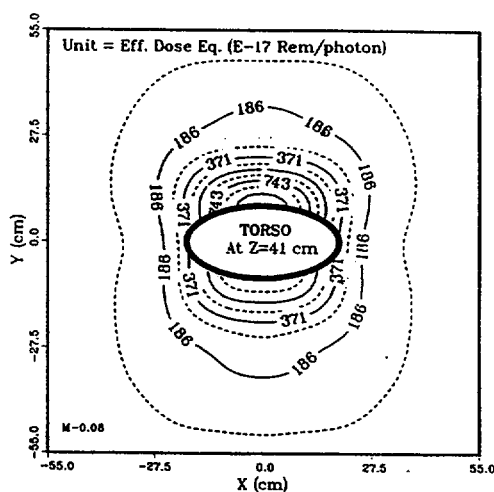
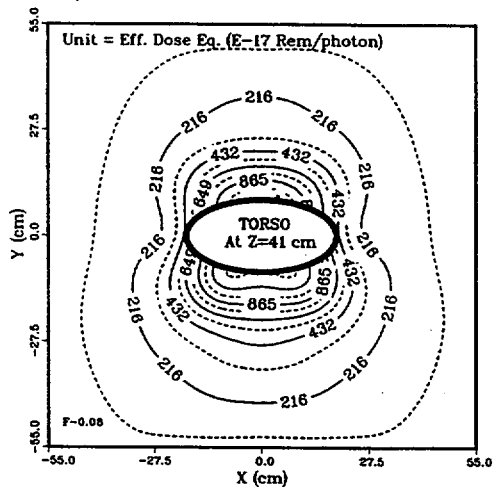
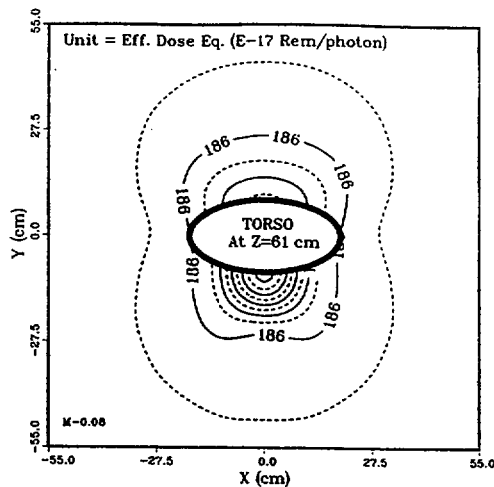
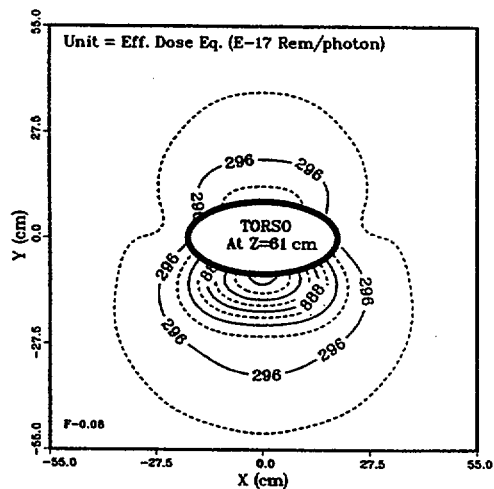
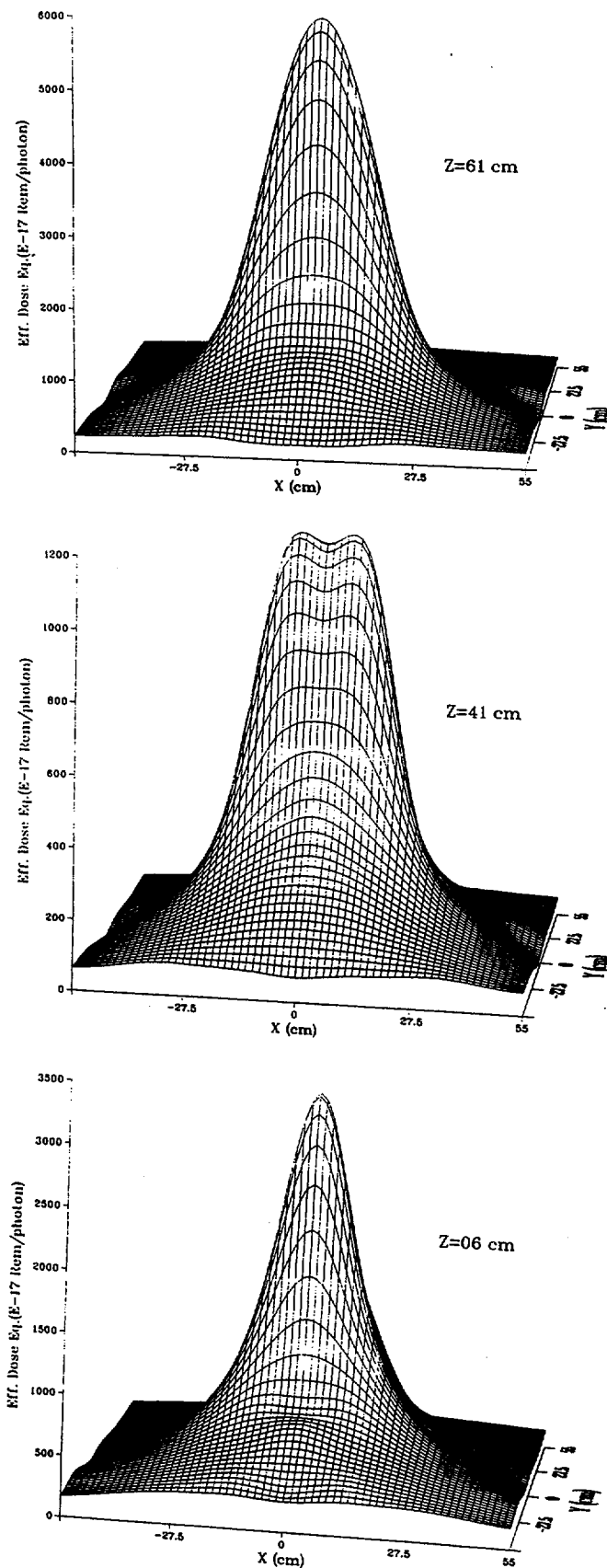


Figure A1-9. Contour plots of H_E for a female vs. source location for a 0.08 MeV point source

Figure A1-10. Contour plots of H_E for a male vs. source location for a 0.08 MeV point source



A1-20

Figure A1-11. Surface plots of H_E for a female vs. source location for a 0.3 MeV point source

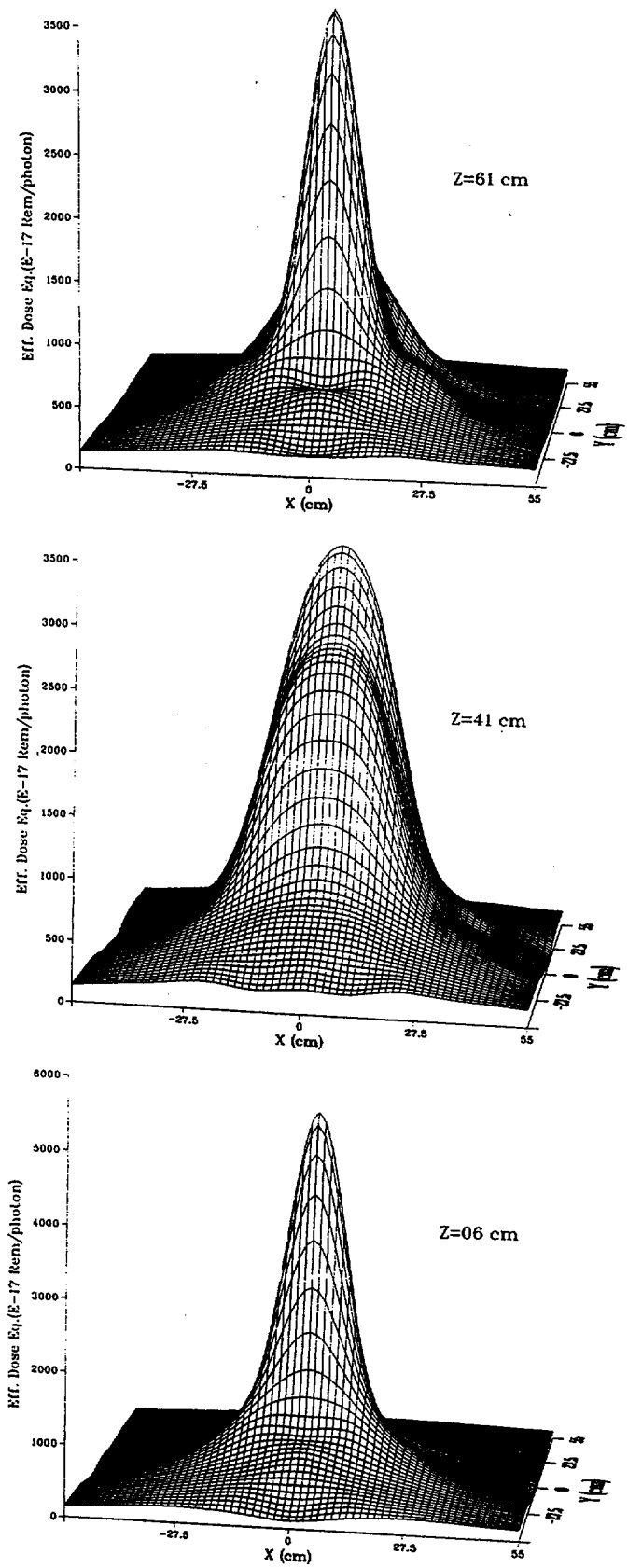


Figure A1-12. Surface plots of H_E for a male vs. source location for a 0.3 MeV point source

About EPRI

EPRI creates science and technology solutions for the global energy and energy services industry. U.S. electric utilities established the Electric Power Research Institute in 1973 as a nonprofit research consortium for the benefit of utility members, their customers, and society. Now known simply as EPRI, the company provides a wide range of innovative products and services to more than 1000 energy-related organizations in 40 countries. EPRI's multidisciplinary team of scientists and engineers draws on a worldwide network of technical and business expertise to help solve today's toughest energy and environmental problems.

EPRI. Powering Progress

© 1999 Electric Power Research Institute (EPRI), Inc. All rights reserved. Electric Power Research Institute and EPRI are registered service marks of the Electric Power Research Institute, Inc. EPRI. POWERING PROGRESS is a service mark of the Electric Power Research Institute, Inc.

 Printed on recycled paper in the United States of America

EPRI • 3412 Hillview Avenue, Palo Alto, California 94304 • PO Box 10412, Palo Alto, California 94303 • USA
800.313.3774 • 650.855.2121 • askepri@epri.com • www.epri.com